NUREG/CR-2189, Vol. 6
UCID-18967, Vol. 6
RM

# Probability of Pipe Fracture in the Primary Coolant Loop of a PWR Plant

NUREG/CR--2189-Vol.6
TI85 016042

## Volume 6: Failure Mode Analysis Load Combination Program Project I Final Report

Manuscript Completed: June 1981
Date Published:

Prepared by

R. D. Streit

**Lawrence Livermore Laboratory**
**7000 East Avenue**
**Livermore, CA 94550**

**Prepared for**

**Division of Engineering Technology**
**Office of Nuclear Regulatory Research**
**U.S. Nuclear Regulatory Commission**
**Washington, D.C. 20555**
**NRC FIN No. A-0133**

---

Blank Page

## ABSTRACT

Material properties and failure criteria were evaluated to assess the requirements for double-ended guillotine break in the primary coolant loop of the Zion Unit 1 pressurized water reactor. The properties of the 316 stainless steel piping materials were obtained from the literature. Statistical distributions of both the tensile and fracture properties at room and operating temperatures were developed. Yield and ultimate strength tensile properties were combined to estimate the material flow strength. The flow strength and fracture properties were used in the various failure models analyzed. Linear-elastic, elastic-plastic, and fully plastic fracture models were compared, and the governing fracture criterion was determined. For the particular case studied, the fully plastic flow requirement was found to be the controlling fracture criterion leading to a double-ended guillotine pipe break.

CONTENTS

LIST OF FIGURES

## LIST OF TABLES

# EXECUTIVE SUMMARY

The Code of Federal Regulations requires that structures, systems, and components that affect the safe operation of nuclear power plants be designed to withstand combinations of loads that can be expected to result from natural phenomena, normal operating conditions, and postulated accidents. One load combinations requirement--the combination of the most severe LOCA (loss-of-coolant accident) load and SSE (safe shutdown earthquake) loads--has been controversial because both events occur with very low probabilities. This issue became more controversial in recent years because postulated large LOCA and SSE loads were each increased by a factor of 2 or more to account for such phenomena as asymmetric blowdown and because better techniques for defining loading have been developed.

The original objective of Load Combinations Project I was to estimate the joint probability of simultaneous occurrence of both events and to develop a technical basis for the NRC (Nuclear Regulatory Commission) to use in determining whether it could relax its requirement on the combination of SSE and large LOCA for nuclear power plants. However, in the process of probability estimation we have not only estimated the probability of simultaneous occurrence of a large LOCA and an earthquake, but also estimated the probability of a large LOCA caused by normal and abnormal loading conditions without an earthquake. The estimates provide very useful information on the likelihood of asymmetric blowdown, which is a subset of large LOCA. Also, the probabilistic fracture mechanics model that we developed can be used to estimate the probability of pipe rupture with or without prior leak. That is, we can estimate the proportion of pipes that will leak detectably before rupture under normal operation, accident, or upset conditions. We can also evaluate the piping reliability in general. After a sufficient parametric study is done, we will be able to recommend a more rational basis for postulating pipe rupture locations.

If earthquakes and large LOCAs are independent events, the probability of their simultaneous occurrence is small. However, this probability is expected to be greater if an earthquake can induce pipe failure that leads to a LOCA. This LOCA could result directly (i.e, ground motion causes a pipe break in the primary cooling system) or indirectly (e.g., an earthquake causes a structural, mechanical, or electrical failure that in turn causes a pipe break in the primary cooling system).

In the first-phase study reported in these nine volumes, we concentrated on determining the probability of a large LOCA in a PWR plant directly induced by an earthquake. The expert consensus is that such a directly induced LOCA is most likely to result from the growth of cracks formed in the pipes during fabrication. We selected a demonstration plant for study (Unit 1 of the Zion Nuclear Power Plant), modeled its primary cooling loop (Vol. 2), analyzed the best estimated responses of that piping system to non seismic and seismic stresses (Vols. 3 and 4), developed a probabilistic fracture mechanics model of that piping system (Vols. 5, 6, and 7), analyzed the failure modes (Vol. 6) and developed a computer code, PRAISE, to simulate the life history of a primary coolant system (Vol. 9). Finally, we examined the probability with which an earthquake can indirectly induce a LOCA (Vol. 8).

In Volume 6, we develop a failure mode analysis. The relation between this volume and the rest of the report is shown in the following schematic:

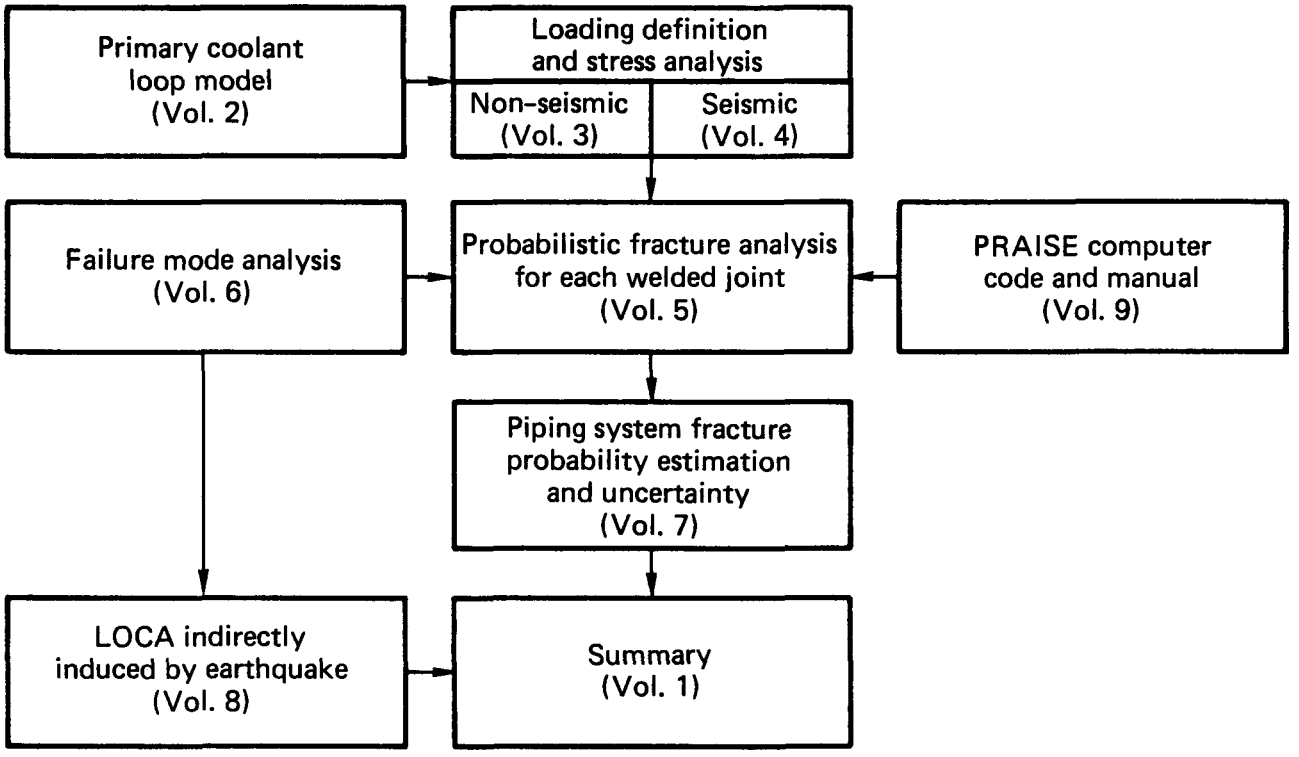

# 1.0 INTRODUCTION

A double-ended guillotine break in the primary coolant loop of a pressurized water reactor (PWR) is one of the extreme accident events the PWR system must be designed to withstand. While the consequences of such an accident have been analyzed in numerous studies, the conditions leading to this accident have only recently come under investigation. The loading on the primary coolant loop pipe, the piping material mechanical properties, and the failure model all play an important role in predicting piping failure. In this report we first evaluate the mechanical properties of the coolant pipe and then assess a full range of pipe failure criteria to estimate the critical loading leading to a double-ended pipe break.

The failure mode analysis of the primary coolant loop presented here is part of the Load Combinations Program, Project I, at the Lawrence Livermore National Laboratory. The objective of Project I is to estimate the probability that a double-ended guillotine break in the primary coolant loop and an earthquake occur simultaneously.[1] Because large dynamic loads would result as a consequence of a double-ended guillotine pipe break, only this type of fracture is considered in the current study.

We estimate the probability of pipe break as a function of plant life by considering the growth of cracks due to fatigue. A flaw-size distribution is assumed at the start of plant operation and then updated to account for crack growth resulting from both normal and abnormal operating transients.[2] Failure is presumed to occur when the crack grows to a sufficient size such that the applied load-controlled stresses can sever the degraded pipe. The study is probabilistic; the fatigue and fracture analysis require random inputs of loading and material properties.

The cracks modeled in the primary coolant loop are all in the circumferential orientation because these cracks can lead to a double-ended pipe break (DEPB). Three types of circumferential cracks are evaluated in the Load Combination study:[2] (1) a semi-elliptical internal surface crack, (2) a through-wall crack, and (3) a complete circumferential internal surface crack. Preliminary fatigue and fracture analyses indicate that a semi-elliptical internal surface crack or a through-wall crack will generally result in a leak before becoming a double-ended pipe break.[2] Thus, although important to design, these cracks can be found (with leak detectors or during

inspection) and repaired before complete pipe break. A complete (or nearly complete) circumferential crack, on the other hand, could lead to a DEPB without prior leaking and, thus, without warning. It is the objective of this volume to assess under what loading such an axisymmetric crack will result in a complete pipe severence.

Fracture is assumed to be due to the load-controlled stresses applied to the pipe. The load-controlled stresses are those prescribed independently of the pipe deformation or displacement and thus do not relax as a consequence of crack extension. For the system considered here, the internal pressure is the dominating factor in the stress analysis.[3] Therefore, the failure-mode analysis for the directly induced DEPB is treated as an axisymmetric problem with uniform axial loading. For the analysis of pipe break due to an external load source (i. e.; missle impact), bending moments are the major factor and must be considered.

## 1.1 SCOPE

To assess the critical loading that can lead to a DEPB, both the piping material properties and a range of failure criteria need to be assessed. First, the mechanical properties of the materials used in the primary coolant loop are evaluated. Material properties are considered first because they will establish the limits to which the material can be loaded. The critical fracture load is defined as the minimum load necessary to cause a DEPB on the basis of all applicable failure criteria. It is important to include the influence of the statistical distribution of the pertinent material properties since the investigation is probabilistic. Both tensile and fracture property data are collected, and statistical distributions are presented to describe their random nature. Material property analysis is covered in Section 2.

An appropriate failure criterion is necessary to evaluate the critical loading required to cause a DEPB. In the failure analysis section (Section 3) we consider the loading applied to the pipe and assess at what point the material is loaded to its capacity as defined by the material properties. Since the materials used in reactor primary loop piping are generally very ductile, this evaluation has often been based on plastic-limit-load calculations--i.e., exceeding the material flow strength in the pipe section.

However, in addition the piping system must be safe against unstable crack propagation. Thus, the complete range of failure criteria--linear-elastic, elastic-plastic, and fully plastic--is considered here. We consider both direct loading of the pipe, as necessary for evaluating directly induced DEPB,[2] and loading of the pipe via an external source, as required for evaluating indirectly induced DEPB.[4]

## 1.2 DESCRIPTION OF PIPING

The failure mode analysis is based on an evaluation of the Zion Unit I PWR. Specifically, we are interested in the girth-welded butt joints of the primary coolant loop piping. These weld joints were chosen because of the interest in the double-ended guillotine pipe break as discussed earlier. Such a failure would result if any of these joints were to completely sever. The primary piping includes the hot leg (i.e., reactor pressure vessel to steam generator), crossover leg (i.e., steam generator to coolant pump), and the cold leg (i.e., reactor coolant pump to the reactor pressure vessel) of each of four loops of the primary coolant system. The temperature and pressure in each of these three legs are tabulated in Table 1 along with the nominal piping dimensions.[5] Figure 1 shows a plan view of the piping arrangement; the butt girth welds analyzed in this study are identified. There are 14 girth welds per loop, for a total of 56 possible failure locations. The layout and lengths of the pipe legs are important for assessing the stability of crack propagation should crack growth initiate. A typical length of a hot leg is 150 in. (3.8 m).

The primary piping, nozzles, and fittings are made of various grades of cast and wrought 316 stainless steel.[5] In this study, no attempt is made to differentiate the mechanical properties in these different components. The ASME Code requirements for the minimum specified yield and ultimate strengths at room temperature are 30 ksi (207 MPa) and 70 ksi (483 MPa), respectively. The code-allowable stress at the operating temperature ranges from 11.8 ksi (81 MPa) to 16.8 ksi (116 MPa), depending on whetner piping, fitting, or nozzle material is considered.[6] Estimates of the actual material properties are dealt with in more detail in subsequent sections.

TABLE 1. Nominal pressure, temperature, and dimensions of tne primary piping.[1]

| | Operating pressure psi (kPa) | Temperature $^{o}F$ ($^{o}C$) | Outside diameter in. (cm) | Thickness in. (cm) | Lengtn in. (m) |
|---|---|---|---|---|---|
| Hot leg | 2235 (15400) | 592 (311) | 34.0 (86.4) | 2.50 (6.4) | 151 (3.83) |
| Crossover leg | 2235 (15400) | 530 (277) | 36.3 (92.2) | 2.66 (6.8) | 97 (2.46) |
| Cold leg | 2235 (15400 | 530 (277) | 32.3 (82.0) | 2.38 (6.0) | 223 (5.66) |

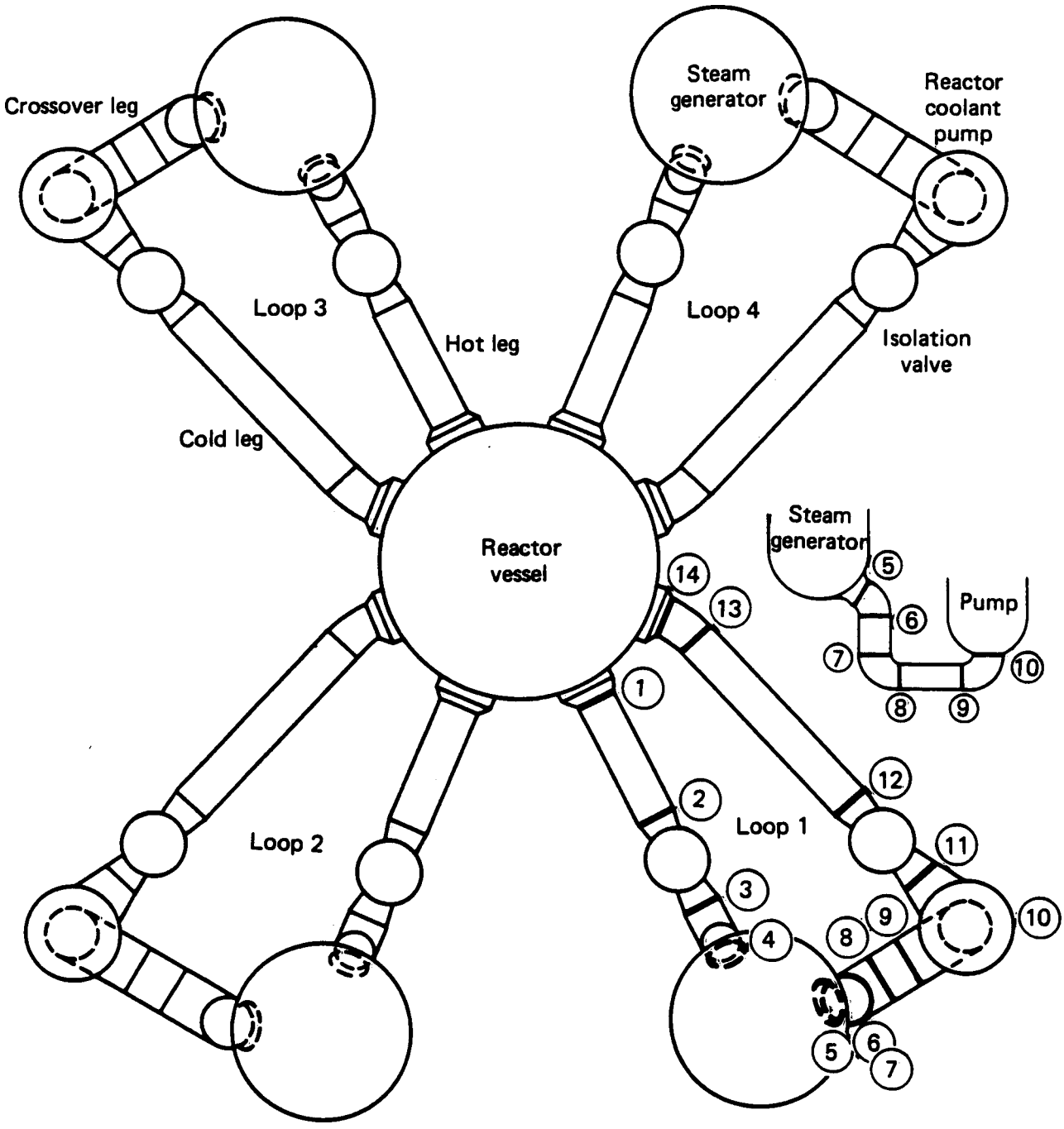


FIG. 1. Diagram of Zion 1 primary piping. The hot-leg pipe, welds 1-4 of loop 1, is analyzed in this failure mode analysis.

## 2.0 MECHANICAL PROPERTY EVALUATION

An understanding of both flow and fracture properties of the primary loop piping material is necessary for evaluating the failure criteria for guillotine pipe break. The critical fracture load is the minimum load that will propagate a circumferential crack, or the load required to reach the plastic limit load in the cracked pipe section. The plastic-limit-load calculations require an estimate of the material flow strength, whereas the crack growth criterion requires knowledge of fracture-mechanics-based material behavior.

The material flow stress can be approximated as the average of the yield and ultimate strengths. This approximation of flow stress takes into account material hardening and has been useful in predicting a net-section plastic-collapse mode of failure.[7,8] Its value is estimated from data on yield and ultimate strengths, which are available in the literature (as will be discussed in detail). The statistical distribution of these properties is considered for input to the probabilistic failure model. Elastic and elastic-plastic fracture models are required in addition to the fully plastic flow criteria to account for the crack-initiation and -growth failure modes. Fracture data, although more limited than the tensile property data, are also collected and presented.

The pipe material is ASTM A-376 Type 316 stainless steel. The fittings and nozzles are ASTM A-351 Grade CF8M and ASTM A-182 Grade F316, respectively.[5] The material in the weld and heat-affected zone are of primary concern because the cracks are postulated to exist in the circumferential butt welds. However, as mechanical property data for welds are very limited, the parent material properties will be employed in conjunction with available weld data. Properties that are evaluated at or near the operating temperature ($550^{o}$-$600^{o}$F) are of particular interest, since crack growth and ultimate failure are assumed to occur during plant operation.

## 2.1 TENSILE PROPERTIES

### 2.1.1 Tensile Properties Measured at Room Temperature

Data on yield strength and ultimate tensile strength of piping materials have generally been obtained at room temperature. Although the values measured at the plant operating temperature will differ from the room-temperature values of the same properties, data taken at room temperature were used to develop an estimation procedure for the distribution of flow strength.

Data are collected for both the yield and ultimate strengths. These data are subsequently used to develop appropriate distributions, which are in turn combined to calculate the flow stress. It would be desirable to obtain data pairs--that is, to measure yield and ultimate strengths from the same specimen. The flow stress could then be calculated by simply computing the average of each pair and, subsequently, the average of the flow stress obtained from all specimens. However, the available data are generally not listed in this manner, and a method of combining the data is necessary.

Histograms for the yield and ultimate strength data of 316 stainless steel--as obtained from many sources in the literature[9-14]--are shown in Figs. 2 and 3. Most of this data has not been obtained from reactor piping material per se, but does represent the various types and grades of 316 stainless steel used in the piping system. On the basis of the nature of the variability of tensile properties[9,10,12,15-18] a normal distribution was chosen to describe the data. The appropriate normal distributions are shown superimposed on the histogram plots in Figs. 2 and 3. These distributions are described by the mean and standard deviation:

| Mean | Standard deviation |
|---|---|
| $S_y^o$ = 36.6 ksi (252 MPa) | $SD_y$ = 6.2 ksi (42.7 MPa) |
| $S_u^o$ = 83.5 ksi (576 MPa) | $SD_u$ = 4.4 ksi (30.3 MPa) |

For comparison, the ASME Code requirements for the minimum specified room-temperature yield and ultimate strengths are 30 ksi (207 MPa) and 70 ksi (483 MPa), respectively.

The ultimate strength is well described by the normal distribution with the exception of a "lack of fit" in the lower strength region. This discrepancy--a lack of lower tensile strength properties--is observed for other materials as well.[9,10,15,16] This is believed to be associated with meeting the minimum strength requirement of the given material specification. By including the lower tail to the normal distribution, we are being somewhat conservative in the estimate of tensile properties. Fig. 2 shows the lack of data in the lower strength region.

In Fig. 3 we observe a rather broad distribution of yield data. The data in the central region do not follow the normal distribution, but rather appear to be uniformly distributed. This behavior is most likely due to the lack of a distinct yield point in 316 stainless steel. Different laboratories will report different yield data for similar material simply because they use different measurement techniques. Thus, variability in yield data is probably related to this inconsistancy in yield point measurement.

The flow stress, approximated as the average of the yield and ultimate strengths, is now evaluated from the distributions obtained for the yield and ultimate tensile strengths. Given that these distributions are normal, and assuming that we can approximate the flow stress distribution as normal, the mean and standard deviation of the flow stress are given by;

$$S_F^o = \frac{S_y^o + S_u^o}{2}$$

and

$$SD_F = \frac{1}{2}\left[(SD_y)^2 + (SD_u)^2 + 2\rho\ (SD_y)\ (SD_u)\right]^{1/2}$$

where $S_i^o$ = mean of stress $S_i$ (y = yield, u = ultimate, F = flow)
$SD_i$ = standard deviation of stress $S_i$
$\rho$ = correlation coefficient.

Using the distributions for the data presented in Figs. 2 and 3, we estimate the mean room-temperature flow stress to be 60.2 ksi (415 MPa).

The standard deviation can be calculated if we assume that the yield-strength and ultimate-strength data are completely correlated or uncorrelated by a linear fit. Setting the correlation coefficient $\rho = 1$

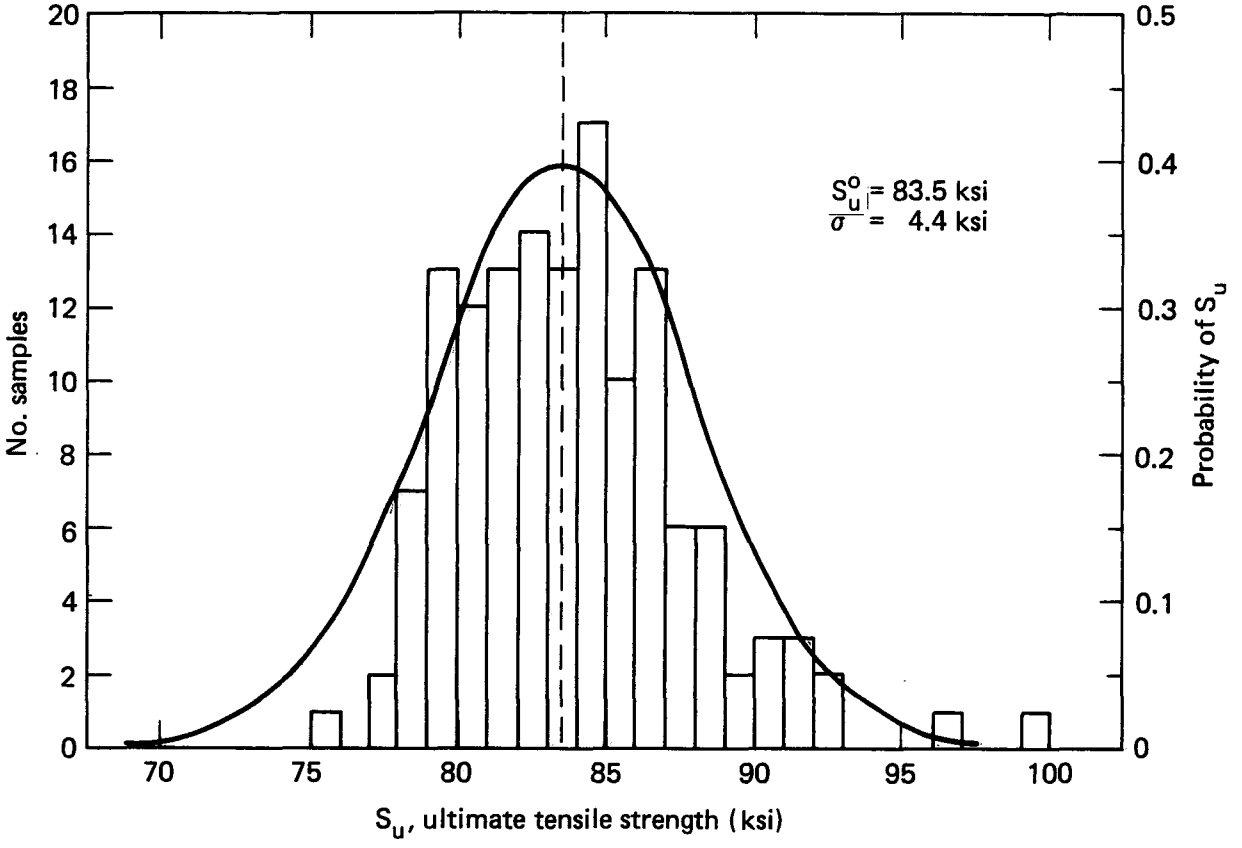


FIG. 2. Histogram of ultimate tensile strengtn data for 316 stainless steel. Normal distribution obtained from data set is snown superimposed. Data were collected from Refs. 9-15.

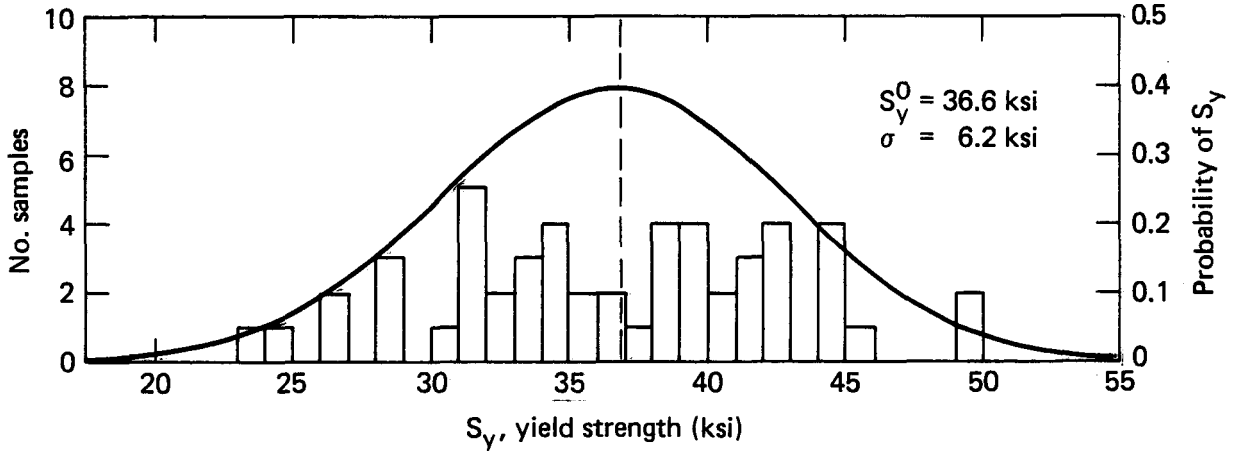


FIG. 3. Histogram of yield strengtn data for 316 stainless steel. Normal distribution obtained from data set is snown superimposed. Data obtained from Refs. 9-15.

means that the two data sets are linearly correlated; whereas, $\rho = 0$ implies that the data are completely uncorrelated by a linear fit. Standard deviation values calculated by these two extremes are

$SD_F$ = 3.8 ksi (26 MPa) if uncorrelated
$SD_F$ = 5.3 ksi (37 MPa) if correlated.

High values of yield strength would correspond to high values of ultimate strength if we assume that the data sets are correlated. If the data sets are uncorrelated, then any yield-strength value could be associated with any ultimate-strength data point. A histogram of data generated from the uncorrelated distribution is shown in Fig. 4. While various arguments can be made as to why the data should or should not be correlated, the correlated value will be employed in the probabilistic analysis.[2]

### 2.1.2 Tensile Properties Measured at Elevated Temperature

The preceding section discussed only properties measured at room temperature and is therefore not representative of properties at PWR operating temperatures. We will make use of the fact that the data appear to be adequately represented by a normal distribution and that the distribution can be combined as previously discussed. Unfortunately, though, data on the tensile properties of the piping material at the operating temperatures (500-600°F, 260-316°C) are very limited.

A literature search of the mechanical behavior of 316 stainless steel at elevated temperatures, however, indicates that the tensile properties recorded in the temperature range of 400-800°F (204-427°C) result in essentially the same estimate of the ultimate strength.[10,12] This trend is shown in Fig. 5. The yield strength does exhibit a slight reduction for test temperatures increasing from 400°F (204°C) to 800°F (427°C), but this reduction is generally less than the scatter observed in the data. Because this range covers all extremes of operating temperature, tensile data within this range will be used to assess the flow strength of the piping material.

Data were collected in this temperature range[10,12] and combined by the procedure discussed in the preceding section. Only 14 data points were obtained for each the yield and ultimate strength. These data fell within a

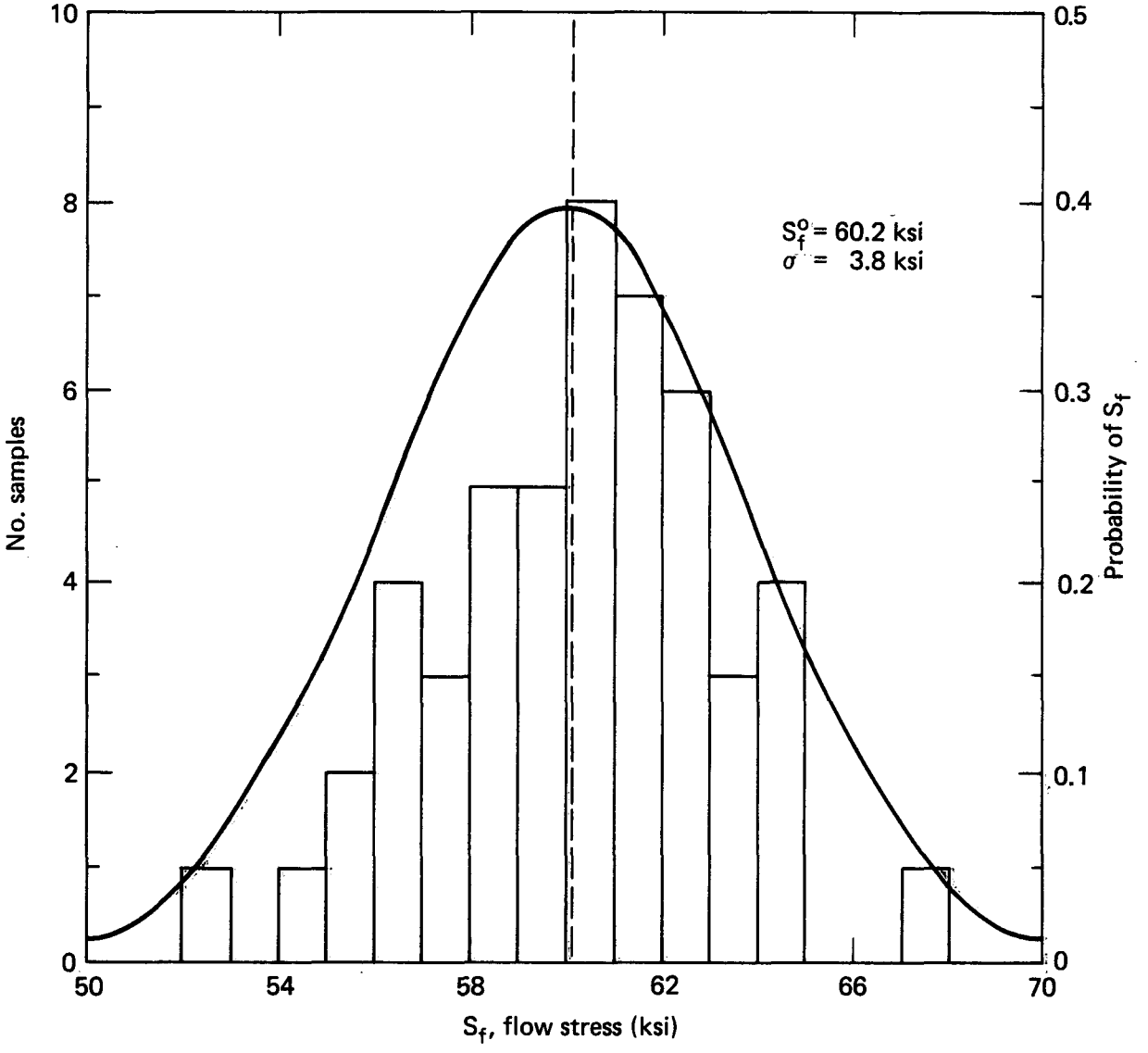


FIG. 4. Flow stress distribution as generated from the distributions for yield and ultimate strength (measured at room temperature) shown Figs. 2 and 3. The assumption is made that the yield and tensile strength are uncorrelated, $\rho = 0$.

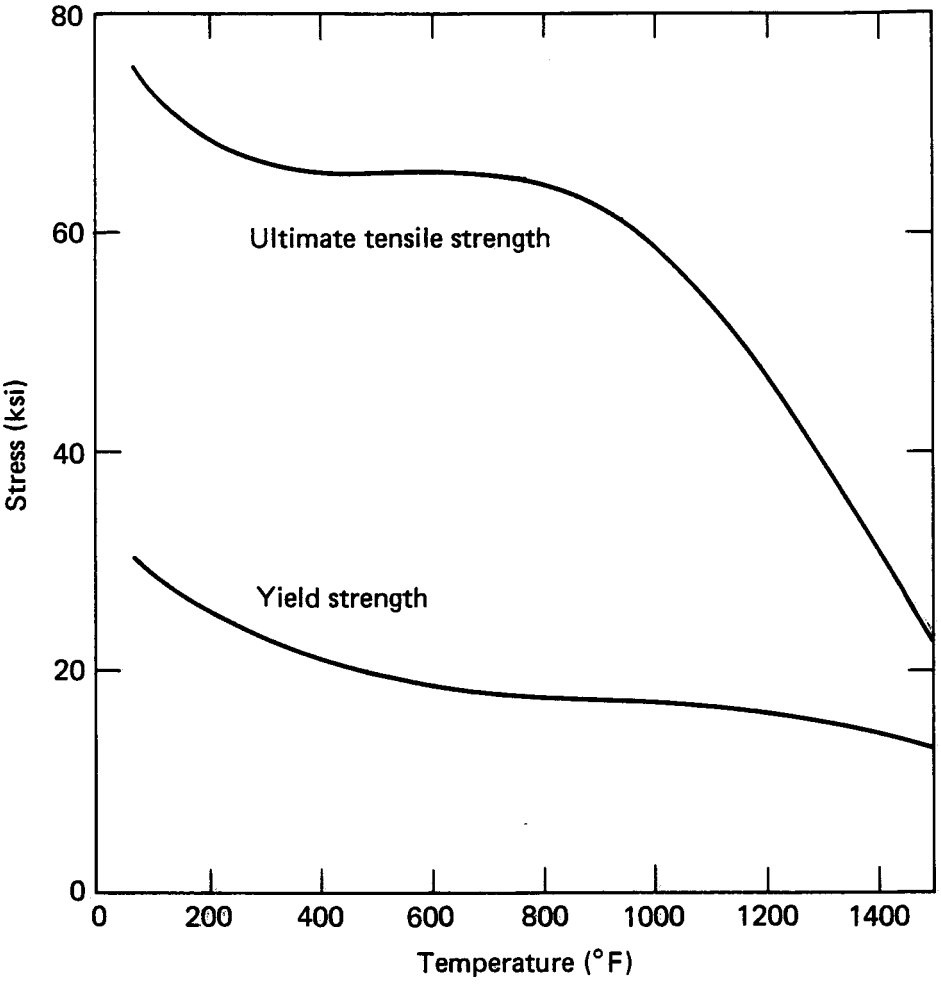


FIG. 5. Effect of temperature on yield strength (0.2% effect) and tensile strength of 316 and 316H stainless steel. Yield and tensile strengths have been adjusted to 30 ksi and 75 ksi at 75°F, respectively, Ref. 11.

rather tight scatter band; the result is a correspondingly low standard deviation. The values for yield, ultimate, and flow strength are:

| Mean | Standard Deviation |
|---|---|
| $S_y^o$ = 21.6 ksi (149 MPa) | $SD_y$ = 1.5 ksi (10.3 MPa) |
| $S_u^o$ = 68.1 ksi (470 MPa) | $SD_u$ = 2.3 ksi (15.9 MPa) |
| $S_F^o$ = 44.9 ksi (310 MPa) | $SD_F$ = 1.9 ksi (13.1 MPa) |

The standard deviation of the flow stress is calculated with the assumption that the yield and ultimate strengths are linearly correlated with $\rho = 1$. These values are used in the probabilistic fracture mechanics evaluation discussed in Volume 5 of this series.[2]

## 2.2 FRACTURE PROPERTIES

An assessment of the materials' fracture behavior is required to evaluate the materials' resistance to crack growth and unstable crack propagation. The fracture properties will be used in addition to the tensile flow properties to determine the critical loading conditions for pipe fracture. As with the tensile properites, it is desirable to develop some statistical distribution of fracture properties for use in the probabilistic analysis.

Fracture properties are generally classed as either linear-elastic or elastic-plastic, depending on the extent of plastic deformation in the vicinity of the crack tip. Linear-elastic fracture mecnanics (LEFM) uses the materials' fracture toughness $K_{Ic}$ to predict the onset of unstable crack propagation. To use this model for fracture prediction, we must constrain the crack tip plastic zone to be on the order of 1/50 the crack or component dimensions.

Elastic-plastic fracture mechanics (EPFM) accounts for plastic deformation as restricted by the deformation theory of plasticity. The plastic zone size limitations placed on fracture testing and design with LEFM can be relaxed signficantly by using elastic-plastic fracture methodology. Various concepts can be employed in EPFM, i.e., J-integral, crack opening displacement (COD), or crack opening angle (COA). On the basis of available data and failure mode analysis employed, tne J-integral will be used.[19] The

elastic-plastic fracture toughness measure for the onset of crack growth is $J_{Ic}$. As the crack starts to grow, the required value of J for continued propagation can increase to many times $J_{Ic}$, depending upon the material, loading, and specimen geometry. This increase in J with crack growth is often measured in terms of the slope dJ/da or tearing modulus $(S_F^2/E)$ (dJ/da), as shown in Fig. 6 and discussed on Ref. 20.

The 316 stainless steel piping material is very ductile and tough, and considerable plastic deformation precedes fracture. Elastic-plastic fracture is therefore used to describe its resistance to crack growth. However, because these steels are so tough, it is difficult to obtain valid fracture data, and the available published data are very limited. Using data reported in Refs. 13 and 14 and some unpublisned results obtained at Lawrence Livermore National Laboratory as a basis, we estimate that the room-temperature toughness is about 4000 in.-lb/in.$^2$, whereas the fracture toughness at the PWR primary loop operating temperature of 600°F (316°C) is about one half its room-temperature value; i.e., 2000 in.-lb/in.$^2$. The observed decrease in $J_{Ic}$ with increasing temperature has also been reported for A106 feedwater piping steels[21] and is believed to be due to a change in flow properties. For A106 steel the $J_{Ic}$ value at 425°F (218°C) is 44% of the room-temperature toughness.

The tearing modulus reported for 316 stainless steel ranges from 200 to greater than 600, depending on the type of specimen and test temperature.[13,14] The low values (around 200) correspond to tests at the operating temperature.

There is insufficient data on the fracture behavior of 316 stainless steel to obtain a statistical distribution. The variation of fracture properties of some other steels used in the PWR industry (i.e., A533 and A106) has been discussed.[21,22] The standard deviation for these materials range between 10 and 25% of the mean value. We assume, on the basis of this data and the knowledge that measuring the toughness in stainless steels is difficult and has a high scatter, that the standard deviation will be about 25% of the mean fracture toughness value. The fracture properties along with the corresponding tensile properties are summarized in Table 2.

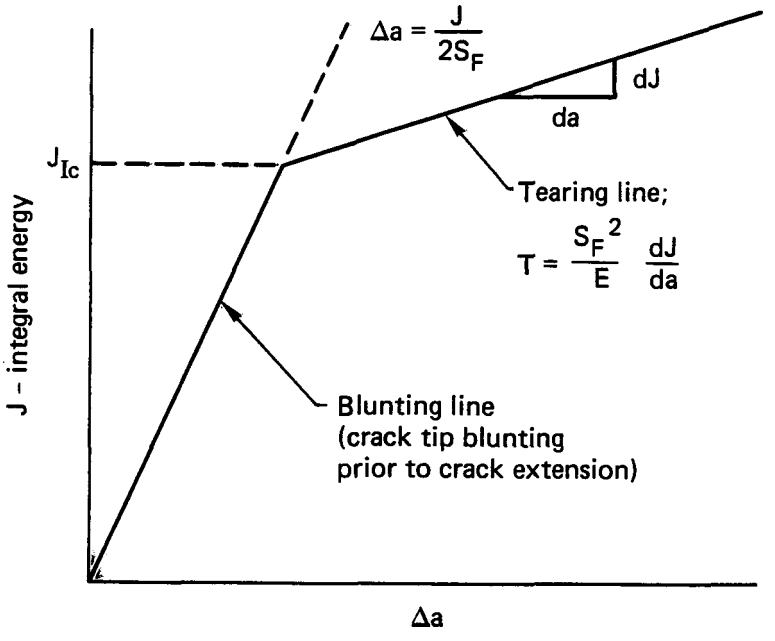


FIG. 6. Schematic representation of J-integral R curve.

TABLE 2. Mechanical properties of 316 stainless steel.

| Property (S.D.)[a] Temp. | Yield strength (ksi) | Ultimate strength (ksi) | Flow stress (ksi) | Fracture toughness (in.-lb/in.$^2$) | Tearing modulus |
|---|---|---|---|---|---|
| Room temperature | $S_y^o$ = 36.6 (S.D. = 6.2) | $S_u^o$ = 83.5 (S.D. = 4.4) | $S_F^o$ = 60.2 (S.D. = 3.8) | $J_{Ic}^o$ = 4000 (S.D. = 1000) | ~350 |
| 500-600°F | $S_y^o$ = 21.6 (S.D. = 1.5) | $S_u^o$ = 68.1 (S.D. = 2.3) | $S_F^o$ = 44.9 (S.D. = 1.9) | $J_{Ic}^o$ = 2000 (S.D. = 500) | ~225 |

[a]Standard deviation

# 3.0 GUILLOTINE PIPE BREAK FAILURE ANALYSIS

A double-ended guillotine break in the primary coolant loop of a PWR is a postulated loss-of-coolant accident that can result in extreme dynamic loads (i.e., the asymmetric blowdown load) on the reactor pressure vessel (RPV) and vessel internals. Various failure criteria have been developed and applied to different piping systems. However, only that criterion yielding the most critical design requirement (i.e., lowest applied loading) is appropriate to the prediction of piping failure. Thus, for different pipes and piping systems the critical failure criteria can vary depending on the material, loading, and pipe and system geometry. Further, when piping reliability is evaluated during plant life, the possibility of damaged or flawed pipes must also be considered.

Different failure modes (i.e., gross plastic yielding, unstable crack growth, and tearing) that can lead to a guillotine pipe break are evaluated in this section. A model for each of the different modes of failure is applied to a primary coolant loop pipe. The pipe is assumed to have a complete circumferential flaw whose depth ranges from virtually zero to 90% through the pipe wall. The complete circumferential crack was chosen because it can lead to the postulated guillotine pipe break without prior leaking (discussed in Section 1).

The principal loading on the primary loop piping system of Zion Unit I is a result of the internal pressure[3]--thus giving rise to a uniform axial loading. Although dead weight and seismic loads do result in bending moment stresses, they are relatively small compared with the pressure stress. The maximum bending moment stress due to these loads is simply considered as an addition to the axial stress due to pressure. Further, axial loading can lead to a guillotine pipe break without first causing a leak. A bending stress may first lead to a leak and therefore provide warning of imminent failure.

In this investigation we evaluate the loading conditions that will cause the hot-leg pipe of Zion Unit 1 to fracture. This piping leg of the primary coolant loop was chosen as a typical example. The hot-leg to reactor-pressure-vessel joint is also one of the most highly stressed joints in the loop. The pipe has a 29 in. (73.7 cm) I.D. with a wall thickness of 2.5 in. (6.35 cm). The mechanical properties of the piping material were discussed in the previous section.

## 3.1 PIPE FAILURE MODELS

Failure models for linear-elastic, elastic-plastic, and fully plastic material behavior are evaluated and compared. By examining these failure models we account for fracture modes ranging from unstable elastic crack propagation to gross plastic tearing in the cracked pipe section. The failure models are compared with each other by assessing which model has the lowest load to fracture. The loading requirement for both the linear-elastic fracture model and the elastic-plastic fracture model is contrasted with the load requirement for plastic flow in the cracked pipe section. In this way the three criteria are compared and the critical criterion chosen.

Since plastic flow will be used as a tool for comparison of the fracture models, it will be useful to discuss this criterion first. Plastic flow is predicted when the average stress in the remaining ligament of a cracked pipe section equals or exceeds the material flow stress, $S_F$.[7,8] This criterion can be written as

$$\sigma_n \geq \frac{A_u}{A_n} S_F$$

where $\sigma_n$ is the nominal stress applied to the pipe, $A_u$ is the area of the remaining ligament of the cracked pipe section and $A_n$ is the nominal pipe area. The flow stress, defined as the average of the 0.2% offset yield and ultimate strength, is discussed in the previous section. With the available data for 316 stainless steel as a basis, we can calculate that flow stress is 60.2 ksi (4.15 MPa) at room temperature and 44.9 ksi (310 MPa) at the PWR operating temperature .

The linear-elastic pipe failure model employs linear-elastic fracture mechanics (LEFM); LEFM concepts predict fracture when the applied stress intensity, $K_I$, equals or exceeds the material fracture toughness $K_{Ic}$; i.e.,

$$K_I \geq K_{Ic} .$$

The applied stress intensity is a function of the pipe and crack geometry, the crack length, and the applied loading. It is evaluated for varying crack depths and for loads up to yielding in the remaining ligament. The stress intensity for the circumferentially cracked pipe geometry is shown in

Fig. 7.[23] The fracture toughness $K_{Ic}$ is approximately 350 ksi-in.$^{1/2}$ (380 MPa-m$^{1/2}$) for the 316 primary piping material at room temperature and about 245 ksi-in.$^{1/2}$ (270 MPa-m$^{1/2}$) at the reactor operating temperature.

LEFM concepts are useful for predicting fracture providing that the extent of plastic deformation in the vicinity of the crack tip is limited. As a rule of thumb, the crack tip plastic zone should be less than 1/50 the crack and thickness dimensions. When the average stress in the remaining ligament approaches the yield strength, LEFM methods are no longer applicable. Thus, if the applied stress intensity has not reached $K_{Ic}$ prior to the average remaining-ligament stress reaching the flow stress, linear behavior will not govern fracture.

A criterion that bridges the gap between linear-elastic and fully plastic material behavior is required. The J-integral fracture criteria is based on elastic-plastic material behavior. It will be employed in cases where linear elasticity can no longer be applied, but a fracture-mechanics-based criterion is still required.

The J-integral, originally defined by Rice,[24] is a path-independent line integral. It can be used to describe the nature of the stress and strain fields in the vicinity of a crack for a power law strain hardening material.[25,26] Using this analysis, McClintock[27] concluded that J is a measure of the plastic stress and strain singularity near the tip of a crack. With such an interpretation, we may regard the field-characterizing parameter J, for the plastic case, as analogous to the stress intensity factor, K, in LEFM. In the linear-elastic range, J, is equal to the crack driving force and, as a result, the critical value of J (i.e., $J_{Ic}$) is related to the plane strain fracture toughness by:

$$J_{Ic} = \frac{1 - \nu^2}{E} K_{Ic}^2 ,$$

where $\nu$ is Poisson's ratio and E is the elastic modulus.

Rice[24] has further shown that the J-integral can be interpreted as the difference in potential energy between two identically loaded plane bodies having infinitesimally differing crack depths, da:

$$J = - \frac{1}{B} \frac{d(PE)}{da} \qquad (3.1)$$

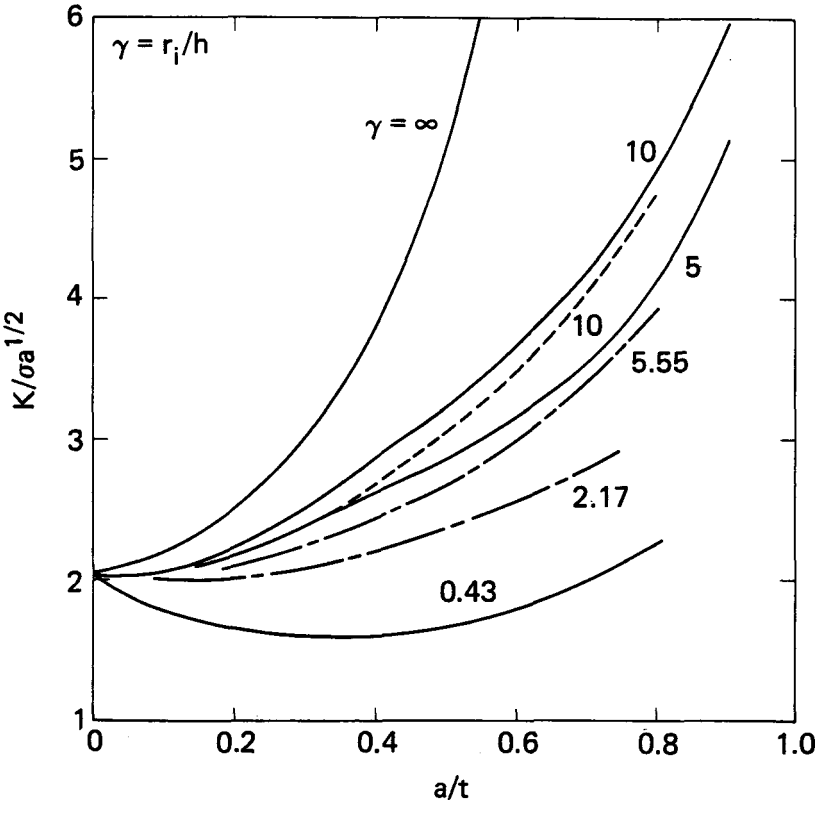


FIG. 7. A comparison of stress intensity solutions for internal surface circumferential cracks in pipes subjected to uniform axial stress.[23] For the Zion 1 nozzle leg, $\gamma = 5.8$ and thus the solution for $\gamma = 5$ will be employed in the linear-elastic analysis.

where PE is the potential energy in a cracked body, a is the crack depth and B the component thickness. The term Bda is thus the infinitesimal difference in crack area. Using this energy definition, Begley and Landes[19,28] proposed the J-integral as a fracture criterion for elastic-plastic behavior of metals. It attempts to extend LEFM concepts to cases in which large-scale plasticity is involved. This energy interpretation of J is shown graphically in Fig. 8. J can be evaluated as a function of load point displacement by measuring the difference in energy between specimens differing only in crack length. The critical value of J is taken at the point of crack initiation and is labeled $J_{Ic}$.

While this criteria is sufficient to predict the onset of crack growth, it does not provide sufficient information to state whether crack growth will be stable or unstable. The slope of the J vs crack extension curve is often employed to predict the stability of cracking for elastic-plastic material behavior. The slope of the J-$\Delta a$ curve gives a measure of the increased resistance to crack extension once the crack has started to propagate. The J-$\Delta a$ slope is often referred to in terms of the tearing modulus,

$$T = S_F^2/E \left(\frac{dJ}{da}\right) .$$

Thus, to get unstable crack propagation in the regime of elastic-plastic material behavior, both initiation and propagation criteria must be met:

$$J_{applied} \geq J_{Ic}$$

and

$$T_{applied} > T_{material} .$$

In the subsequent analysis, we will initially examine the first of these criteria. If this criterion is met, then a tearing analysis will also be required.

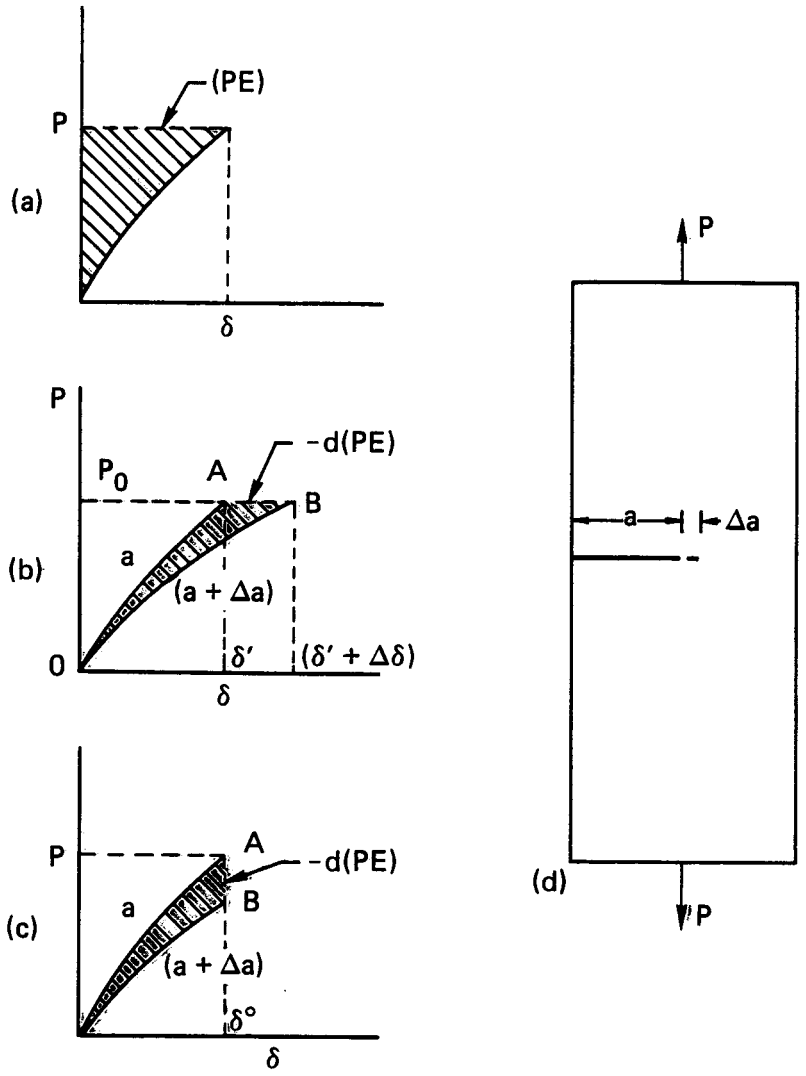


FIG. 8. Generalized load-deflection diagrams employed in the evaluation of J based on the difference in energy (PE). J is calculated from the change in potential energy between two cracked bodies differing only in crack length, Δa.

## 3.2 COMPARISON OF LINEAR-ELASTIC AND PLASTIC FLOW FAILURE MODELS

The linear-elastic fracture criterion was compared with the plastic flow criterion to determine which will govern the material response. Although 316 is very ductile and generally exhibits large plastic deformation prior to failure, this analysis is useful in that it provides information on whether failure of a circumferential crack occurs when the material is within the linear-elastic regime or after gross yielding. The linear analysis also provides a limiting case with which the more complex elastic-plastic fracture behavior can be compared.

In Fig. 9 the stress intensity for a circumferential crack in the Zion Unit I hot leg is shown. It is made nondimensional and presented as a function of normalized crack depth. On the left hand side of Fig. 9 the stress intensity is made nondimensional with respect to the stress applied away from the cracked section. For a stress equal to the minimum material yield strength of 30 ksi (207 MPa) applied to the uncracked pipe section we find that $K_I$ approaches $K_{Ic}$ (approximately 350 ksi-in.$^{1/2}$, 380 MPa-m$^{1/2}$, as calculated from $J_{Ic}$ data) only for very long cracks. Under these conditions the stress on the remaining ligament of the cracked section is many times the material flow stress and, thus, failure is due to an elastic-plastic or fully plastic criterion. The right side of Fig. 9 shows the nondimensional stress intensity for the condition that the stress in the remaining ligament equals the material flow stress. We observe that cracks 40-60% through the pipe wall actually give the highest relative stress intensity. However, even in this regime the stress intensity is many times less than $K_{Ic}$. For a room-temperature flow stress of 60.2 ksi (415 MPa), a fracture toughness of 350 ksi-in.$^{1/2}$ (380 MPa-m$^{1/2}$) and a pipe thickness of 2.5 in. (6.35 cm), the relative stress intensity must exceed 13.5 for LEFM-controlled fracture. For operating-temperture properties (i.e., $K_{Ic}$ = 245 ksi-in.$^{1/2}$, 270 MPa-M$^{1/2}$ and $S_F$ = 44.9 ksi, 310 MPa) the relative stress intensity must exceed 11.9. Values on the order of unity (shown on the right of Fig. 9) are substantially below the requirement of 13.5 or 11.9 for room-temperature or operating-temperature fracture. The rapid decrease in the nondimensional stress intensity beyond 0.6 (a/t) reflects the large reduction in crack area relative to the uncracked section. Thus, due to the hign toughness of 316 stainless steel, linear elastic fracture mechanics is not applicable to the

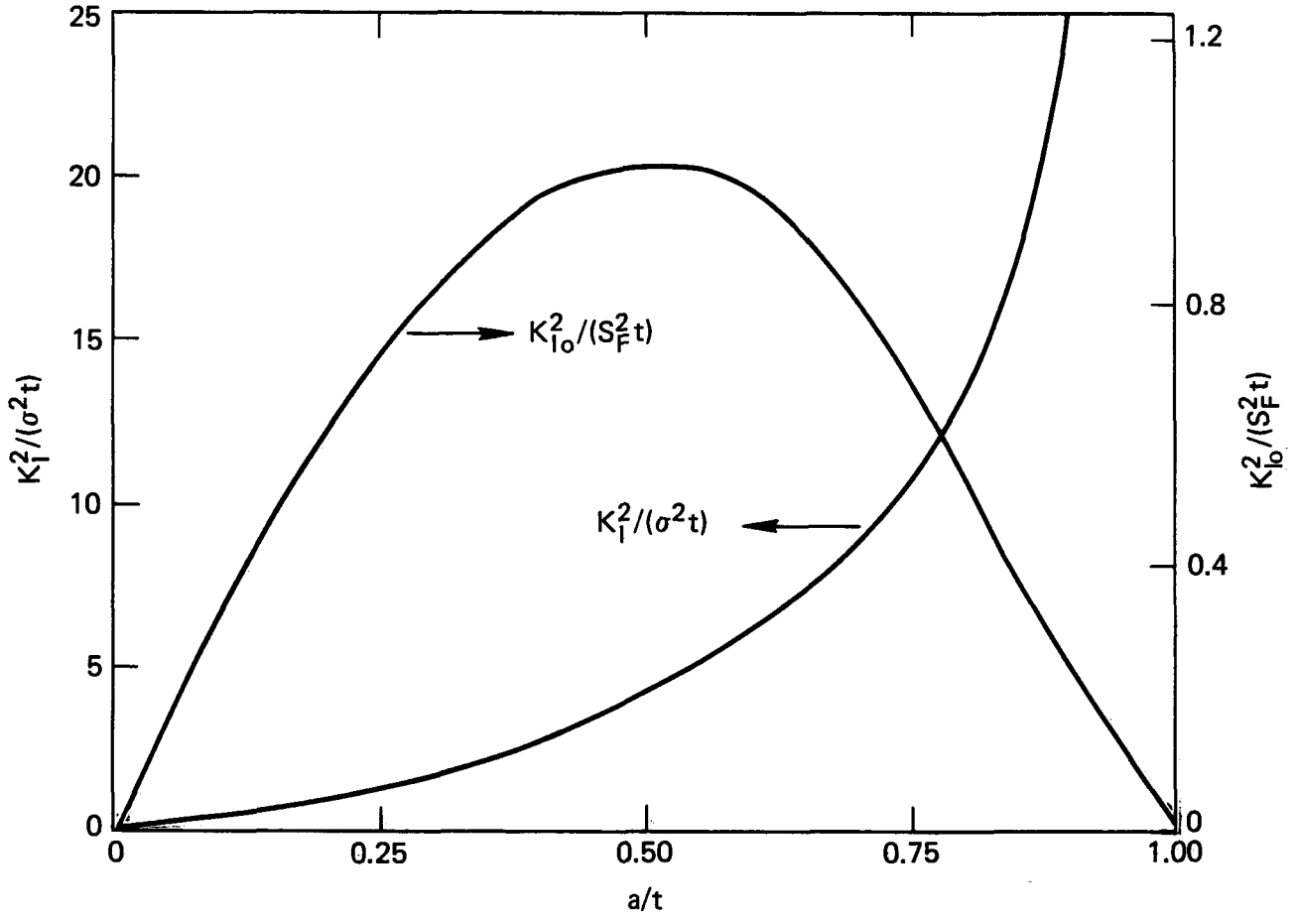


FIG. 9. Linear-elastic stress intensity as a function of crack depth for a complete internal circumferential crack in a pipe with r/t = 5 loaded by a uniform axial load. On the left the stress intensity is made non-dimensional with the applied load and pipe thickness. The right side shows the non-dimensional stress intensity for an applied load giving a stress on the remaining ligament equal to the material flow stress, $S_F$.

pipe fracture problem considered here. However, it should be noted that this may not always be the case for other pipe materials or geometries.

## 3.3 COMPARISON OF ELASTIC-PLASTIC AND PLASTIC FLOW FAILURE MODELS

Since LEFM is not applicable to the pipe fracture problem discussed in this volume, the critical fracture initiation criteria is assessed by comparing the value of the J-integral to $J_{Ic}$ when the stress in the remaining ligament equals $S_F$. The evaluation of J employs a form of the potential energy definition (Eq. 3.1) as given in Eq. 3.2:

$$J = \frac{1}{B} \int_0^P \frac{\partial \Delta(p,a)}{\partial a} dp \ , \tag{3.2}$$

where P is the applied load and $\Delta$ the pipe end displacement. In this formulation the change in potential energy between pipes with crack depths a and (a + da) is evaluated for fixed load as shown in Fig. 8b. The area between the load-deflection curves is estimated and, in turn, J is calculated.

Stress and displacement fields for the circumferentially cracked pipe were calculated using NIKE2D--an implicit finite deformation, finite element code for analyzing two-dimensional elastic-plastic problems.[29] Pipe displacement, as a function of applied load, is tabulated for crack length pairs, $a_m$ and $a_{m+1}$, and J is calculated with an incremental form of Eq. 3.2, as shown in Eq. 3.3:

$$J_i = \frac{1}{2\pi r(a_{m+1} - a_m)} \sum_1^i \Delta P \left[ \frac{\left(\delta_{i+1,m+1} + \delta_{i,m+1}\right)}{2} - \frac{\left(\delta_{i+1,m} + \delta_{i,m}\right)}{2} \right] . \tag{3.3}$$

Here, $J_i$ is the J value at the ith load level and $\delta_{i,m}$ is the pipe displacement at the ith load level with a crack length of $a_m$. The change in crack area is approximated by the pipe circumference at the crack front ($2\pi r$) times the increment of crack extension, $a_{m+1} - a_m$. Although the circumferential crack analysis is not a "truly" plane problem, the axisymmetric correction is small due to the relatively large pipe diameter. A schematic representation of this incremental analysis is shown in Fig. 10.

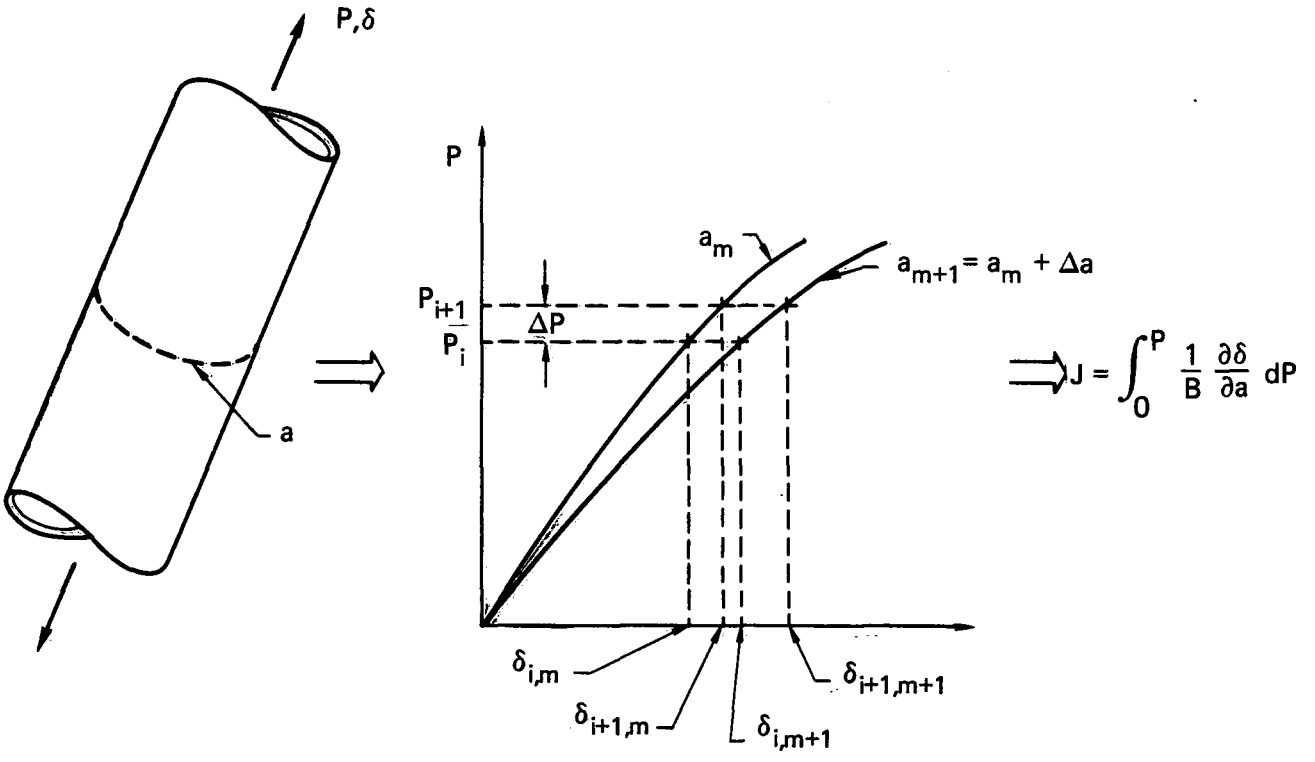


FIG. 10. Schematic representation of the procedure used in the potential energy calculation of the J-integral.

In developing the crack configuration for computer evaluation, care must be exercised to ensure that the load and deflections are indeed representative of the cracked body. Since nigh stress and strain gradients exist near the crack tip, both the element size in the vicinity of the crack and the pipe length must be appropriately chosen. All elements (except for transition elements) are four-noded quadrilateral elements. The minimum element size in the vicinity of the crack was 0.019 in. (0.05 cm) square. Three different finite element zonings of the pipe were used in the analysis--for short, intermediate, and long cracks. In this way the element sizes in the vicinity of tne crack were kept small, whereas we could avoid wasting elements far from the crack without having to rezone for eacn new crack lengtn. No special crack tip elements were used since the displacements were measured remote from the crack tip. Thus while it was important to zone sufficiently fine to maintain the nature of the cracked body, the stress and strain fields at the crack were not used in this evaluation. An example of the zoning is shown in Fig. 11.

The pipe length requirement for the computational analysis was chosen to ensure that the moments induced by the crack attenuated to a very low level on the loading plane. The analysis for a beam on an elastic foundation with an applied moment on one end was employed.[30] A pipe length of 30 in. (76.2 cm) was chosen because this length is sufficient to reduce the moment to less than 1% of its value at the crack plane. The computer analysis confirmed this result; the variation of stress and displacement across the loading plane was insignificant.

The load-deflection behavior must be evaluated for extensive plastic deformation in the cracked section of the pipe. An accurate representation of the material plastic flow behavior is required. Data on the true-stress, true-strain behavior at room temperature was available and was used in the J-integral analysis. At the operating temperatures, both the flow strength and the fracture resistance drop. Thus, while J will reach a critical $J_{Ic}$ at lower loads, the load required to exceed the flow stress in the cracked section will also be reduced. This trade off was observed earlier when we compared the relative stress intensities in the LEFM analysis. A room-temperature stress/strain relation for 316 stainless steel was obtained from tests on standard 0.25-in. (0.635-cm) tensile specimens. The

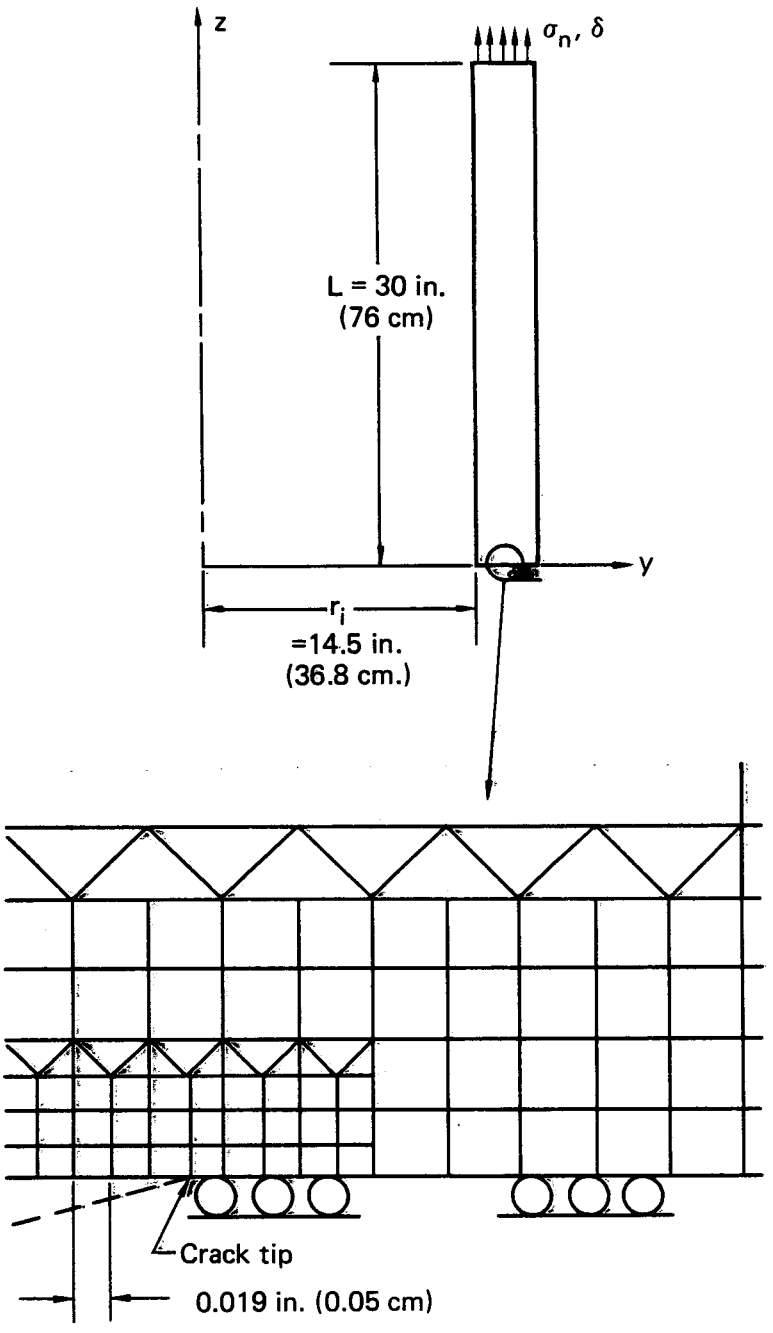


FIG. 11. Pipe model used for elastic-plastic analysis snowing typical zoning in the vicinity of the crack tip.

cross-sectional area of the specimen was monitored as a function of load and subsequently converted into the desired true stress and true-strain, as shown in Fig. 12.

An axial stress was applied to the uncracked end of the pipe in constant incremental load steps. For cracks up to 70% through the pipe wall, a load step of 3000 psi (20.7 MPa) was used. The load step for the deeper cracks was reduced because of the rapid increase in stress in the remaining ligament. Incremental load steps of 2000 psi (13.8 MPa) and 1500 psi (10.3 MPa) were employed for the deeper cracks. All analyses were run to a maximum load of 10 load steps.

At each load step the displacement at the loaded end of the pipe, the nominal stress, and the average stress in the remaining ligament of the cracked pipe section were recorded. The crack length was then incremented by releasing two nodes (approximately 0.040 in., 0.1 cm), and the calculation was rerun. In this way the load-deflection curves for crack length pairs were obtained and used in Eq. (3.3) to obtain J. Subsequently the crack length was increased about 10% of the pipe thickness, and a new pair of data was analyzed.

J is plotted as a function of the applied stress on the pipe in Fig. 13. As expected, the J values at low loads (i.e., within the linear-elastic regime) correlate with the predictions of LEFM. However, as the load (and, in turn, the amount of plasticity) in the vicinity of the crack tip is increased, greater and greater deviations from LEFM are observed. Within this regime of extensive plastic deformation the LEFM solution is a lower bound estimate of J at a given load; i.e., J (elastic-plastic) $\geq$ J (linear-elastic). Since J is proportional to the crack opening displacement and the crack opening displacement resulting from plastic deformation is larger than that due to purely linear-elastic behavior, we would expect this lower bound behavior.

In Fig. 14, J is plotted as a function of the average stress in the remaining ligament of the pipe for various crack depths. For average stresses less than yield in the remaining ligament, the J values remain very low--i.e., less than 5% of $J_{Ic}$. However, as the average stress in the remaining ligament approaches $S_F$, J increases very rapidly. This result is to be expected since the increased plasticity will result in relatively large crack openings and, in turn, large J-integral values. In all cases, however, the critical flow stress was reached before J exceeded the crack initiation $J_{Ic}$ value. Thus, plastic flow in the remaining ligament is the critical failure criteria.

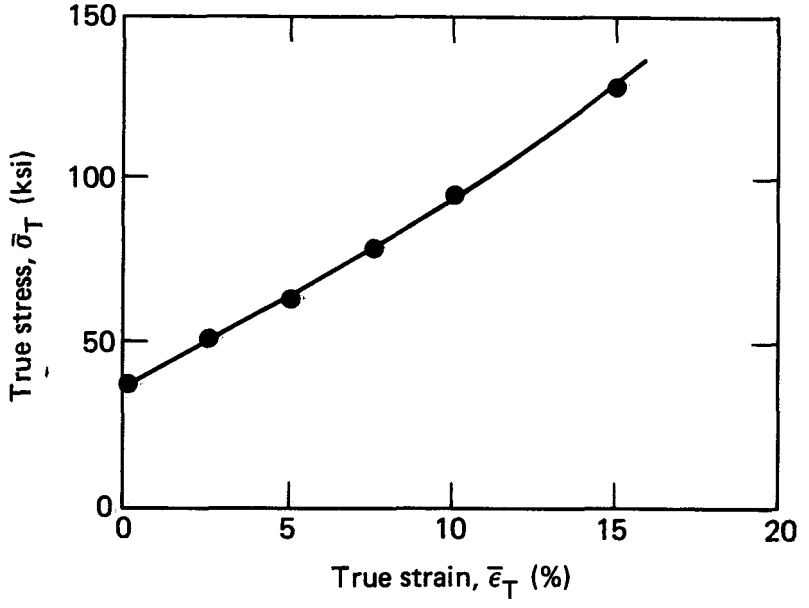


FIG. 12. True stress-strain relation developed from tensile specimens. This material behavior was used as input to NIKE2D for the elastic-plasic analysis.

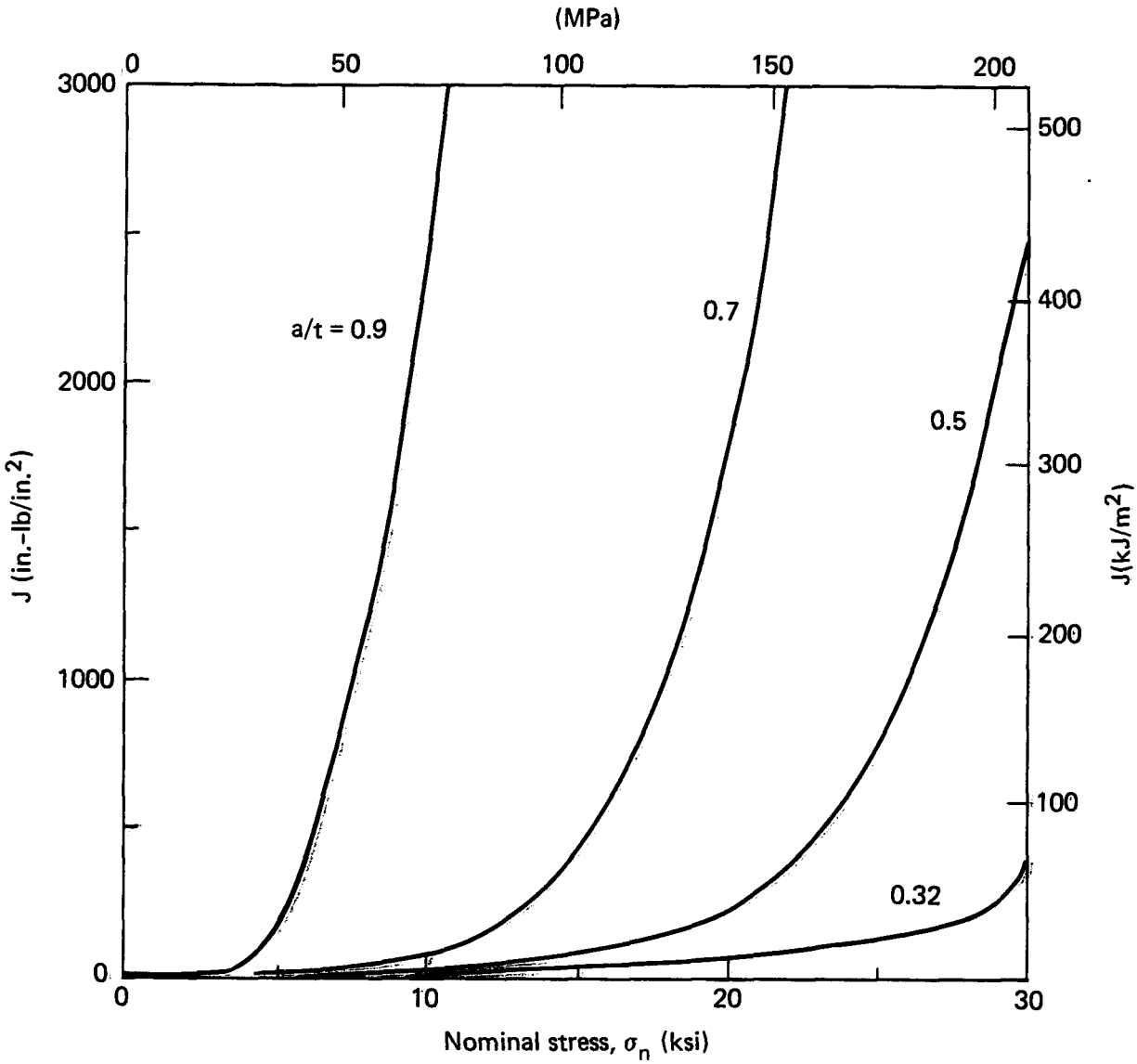


FIG. 13. J for a complete internal crack of deptn a in a pipe as a function of tne applied nominal stress. Tne pipe material is 316 stainless steel witn an i.d. of 29 in. (73.7 cm) and a wall thickness t = 2.5 in. (6.35 cm).

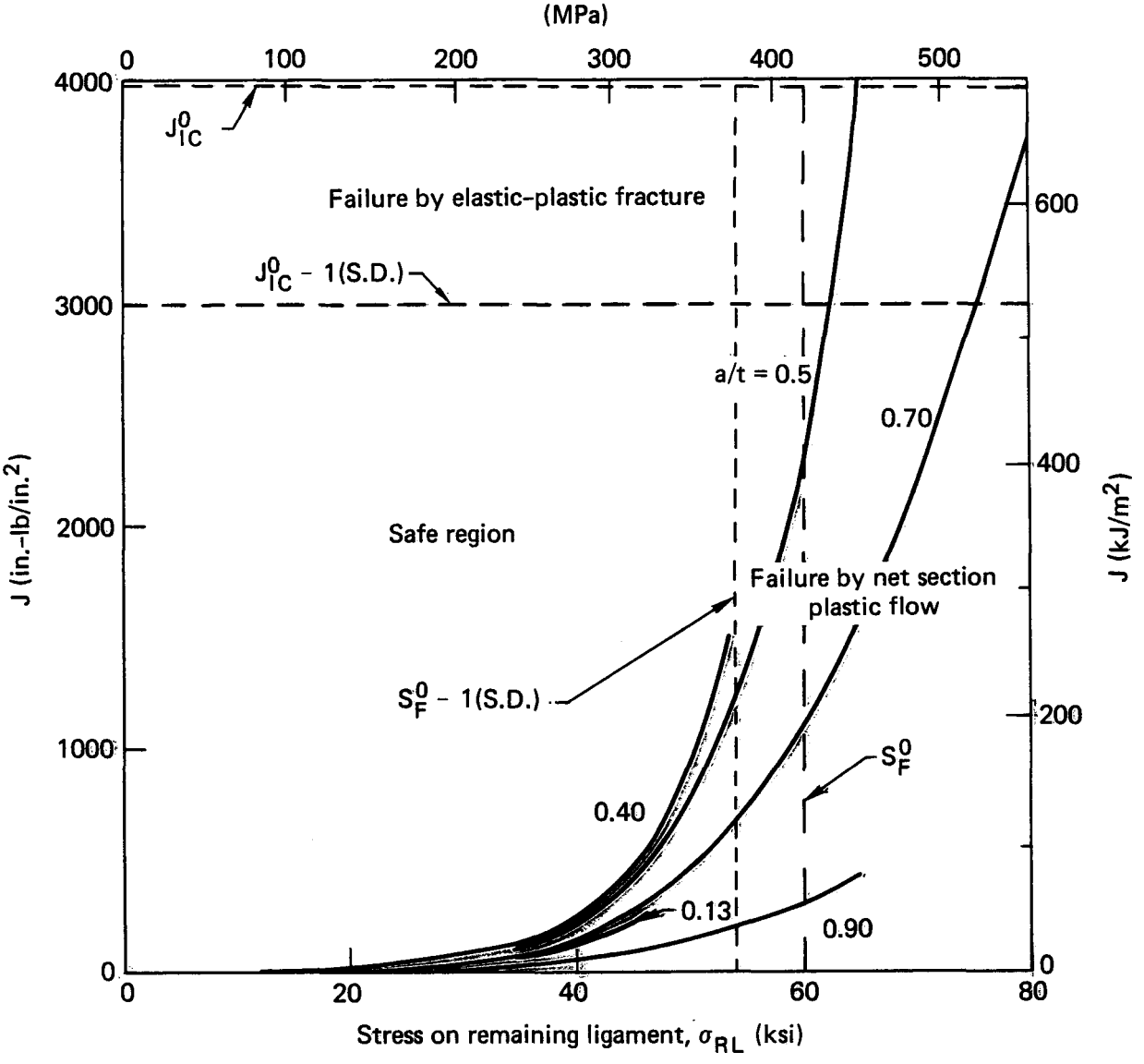


FIG. 14. J for a complete internal circumferential crack (depth a) in a function of the average stress on the remaining ligament. Note that for all cracks the curves cross into the region of failure by net section platic flow prior to reacning the critical elastic-plastic fracture criteria. The pipe is 316 stainless steel with an i.d. Of 29 in. (73.7 cm) and a wall thickness of 2.5 in. (6.35 cm).

It is also interesting to note that the intermediate-length cracks ($0.4 \leq a/t \leq 0.6$) come the closest to reaching the J-integral-controlled fracture criteria. For short cracks J increases with crack length, as expected. As the crack length is increased beyond 60% of the pipe wall, however, the decrease in the area used to calculate stress in the remaining ligament outweighs the increase in crack length. Thus, if the J-controlled criterion is not met for the intermediate length cracks it will not be met for longer cracks. A similar trend was observed for the linear-elastic case as discussed with reference to Fig. 9.

A perfectly plastic estimate of J and tearing was also calculated following the work of Tada, Paris, and Gamble.[31] This was used to establish an upper bound estimate on J and estimate the applied tearing for the reactor coolant loop under consideration. To ensure that these results are compatible with the finite element results presented earlier, the room temperature flow properties will be used; i.e., the flow stress $S_F$ is 60 ksi (414 MPa). In this analysis it is assumed that the cross section containing the crack is fully yielded under an applied bending moment. Under these assumptions J is approximated by:

$$J = S_F \, r \, F_J \, \phi \, ,$$

where r is the mean radius of 15.75 in. (40 cm), $F_J$ is a non-dimensional function of crack geometry and $\phi$ the angle of bending at the crack. For a 50%, through-wall, circumferential crack geometry and a hign axial loading, the factor $F_J$ is about 3.3. The angle $\phi$ can be conservatively estimated by assuming that an elastic moment equivalent to the plastic limit moment is acting over the length of the pipe. The length of the hot leg is about 151 in. (3.8 m). Applying the cooresponding limit moment for the cracked pipe configuration over this length results in an angle of deflection of $3.3 \times 10^{-3}$ radians (or 0.2 degrees). Thus, the plastic limit approximation of J is about 10,000 in.-lb/in.$^2$.

The applied tearing modulus can also be estimated using the perfectly plastic analysis of Ref. 31. From their analysis we obtain

$$T_{appl} = \frac{2}{\pi}\left(1 - \frac{a}{t}\right) F_J^2 \left(\frac{L}{r}\right) + F \frac{JE}{S_F^2 \, r} \, ,$$

where the coefficient F is about -0.19 for the 50%, through-wall, circumferential crack geometry. The $T_{appl}$ is then 32.

Although J values calculated in this way are greater than $J_{Ic}$, the tearing slope was considerably less than estimates of the material tearing resistance. Thus, using this perfectly plastic model, we would conclude that if a crack of sufficient size were present to initiate crack growth, it would be stable and the crack would arrest.

## 3.4 PIPE FAILURE BY INDIRECT LOADING

The requirement for double-ended pipe fracture can be satisified by loading the pipe via an external source; e.g., missile impact. External loading will generally produce bending deflections in the pipe, and thus the axisymmetric elastic-plastic analysis discussed in the previous section is not directly applicable. Regardless of the loading, however, sufficient energy must be made available for the crack to propogate through the pipe wall. The analyses of pipe break from indirect loading is therefore estimated from energy considerations and the details of the stress analysis are not considered.

The energy required for crack initiation per unit area of crack extension is given by $J_{Ic}$. As discussed earlier, the $J_{Ic}$ at the operating temperature is about 2000 in.-lb/in.$^2$ (350 kJ/m$^2$). As the crack begins to grow the required applied J, tne energy for crack growth, increases (see Fig. 6). This increase in J may be many times its initial value. However, for simplicity, let's assume that the "average" energy to propagate a crack (both initiation and growth) is 3000 in.-lb/in.$^2$ (525 kJ/m$^2$). While this value may be somewhat conservative, it does provide a framework on which to base a crack-growth-energy estimate for a DEPB by indirect loading.

Alternatively, the plastic flow failure criteria can be used to estimate the energy required for a DEPB. If the flow stress is exceeded over some critical strain pipe fracture will occur. The load or moment necessary to exceed the flow stress can be calculated by assuming perfectly plastic material behavior with the stress equal to the material flow stress. The limit load $P_L$ is given by the flow stress times the area of the pipe; the plastic limit moment is given by $M_L = 4S_F r^2 t$.

The strain to failure, , is used to calculate a displacement or angle over which the load or moment acts. We assume that failure occurs in a weld

region where the strain to failure is a minimum. For 316 stainless steel, a conservative estimate of the strain to failure is 30%. Taking this strain to act over the weld and heat-affected zone approximately 2 in. (5 cm) long, a required displacement of 0.6 in. (1.52 cm) is estimated. Similarly, the angle $\theta$ is calculated by considering a beam in bending,

$$\theta \approx \frac{\epsilon}{r} \quad .$$

For the hot leg with a radius of 15.75 in. (40 cm), $\theta$ is 0.02 radians or 1.1 degrees.

The area of the pipe, or conversely, the crack size at the location of postulated pipe break is an important factor to consider in calculating the required energy. The uncracked area of the pipe is a function of the crack size distribution, the history of plant operation, and location of indirect loading. The probability that large cracks exist in the pipe is rare.[2] The probability that an indirect load source will contact the pipe at a location where large cracks may exist (i.e., a joint) and that a large crack exists is a combination of two rare events. We thus limit the cracked area to 10% of the nominal pipe area. This will allow for a crack area of about 25 in.$^2$ (160 cm$^2$), or equivalently an uncracked area, $A_u$, of 223 in.$^2$ (1437 cm$^2$) for the hot leg. Given that a crack exists, the probability of a crack of this size is $10^{-5}$ (Ref. 2).

Now, the energy requirements for pipe fracture can be estimated. For a J-controlled fracture the energy for a DEPB is given by

$$E_J = J(A_u)$$
$$= 6.7 \times 10^5 \text{ in.-lb.}$$

The energy requirements for plastic flow are:

$$E_P = P\Delta = (S_F)(A_u)(\Delta)$$
$$= 6 \times 10^6 \text{ in.-lb.}$$

or $$E_M = M\theta = 4(S_F)\,(r)^2\,(t)\,(\theta)$$
$$= 2.2 \times 10^6 \text{ in.-lb.}$$

The minimum requirement is given by the J-controlled growth: $E_J = 6.7 \times 10^5$ in.-lb. ($7.6 \times 10^4$ J).

This energy must be supplied to the cracked section by an external source. However, a failure that generates a missile or other external load source will not necessarily deposit the total energy into the cracked section. We define an inefficiency factor, I, which can be regarded as the ratio of the energy of the missile at the time of pipe impact to the energy input for pipe fracture. Thus, the missile energy must be $(I)(E_J)$ to provide sufficient energy for pipe break.

There are two judgement factors involved with estimating the inefficiency factor.[32] The impact can be of a glancing or rebounding type such that only a fraction of the kinetic energy is directed into the pipe. It is expected that I due to impact efficiency is greater than 2. Secondly, only a portion of the energy that goes into the pipe is expanded directly in causing crack extension. Experience with the study of impact fracture tests (e.g., dynamic tear test and drop-weight tear tests) has shown that no more than half of the drop-weight energy loss goes into work of crack extension. Even with rather rigid supports, half the drop-weight energy is lost in the system (foundation and support strains, vibrations, deformation away from the crack and directly below the impact).[32] On the basis of stated inefficiency inputs, the minimum I is likely to be 4 to 5 with a maximum being "large" such that failure will never occur. Thus, if we consider the minimum inefficiency of 4 with a fracture energy requirement of $6.7 \times 10^5$ in.-lb, the required missile energy is $2.68 \times 10^6$ in.-lb.

The required missile energy can be supplied via a structural failure that results in a falling object ($E = Wh$), or it can result from failure of a moving object. The relation is given by the expression, $E = 1/2\ (W/g)\ v^2$; W is the weight of the missile, h the height of drop, g is gravitational acceleration, and v is the velocity of the missile. To get a feel for the missile size and velocity required, let us consider a 500-lb missile. To achieve the required energy, the missile must impact the pipe at about 170 ft/s or equivalently, drop from a height of 450 ft (137 m). To put this into perspective, tne maximum height from the top of the containment dome to the lowest point on the primary piping (on the crossover leg) is 204 ft (62 m).

In Volume 8 of this series,[4] the various missiles that can be generated inside and out of containment are considered, and the probability of an indirectly induced DEPB is analyzed.

# 4.0 CONCLUSIONS

Mechanical properties of the 316 stainless steel pipe in the primary coolant loop were obtained from the literature. Data were available to obtain the statistical distribution of both the yield and the ultimate tensile strength at room temperature. These values were then combined to obtain an average flow stress of 60.2 psi at room temperature. Using the limited data of tensile properties at elevated temperature, the operating temperature flow stress was approximated to be 44.9 psi. Standard deviations of these properties were also calculated.

Data on the fracture properties of 316 stainless steel were more limited than corresponding tensile properties. Fracture toughness estimates of 4000 in.-lb/in.$^2$ and 2000 in.-lb/in.$^2$ were obtained for the room-temperature and elevated-temperature tests, respectively. The degree of scatter as observed in the standard deviation is considerably larger than that observed in the tensile data. Whether this is due to randomness of the mechanical property (true scatter in the material behavior) or simply to our inability to precisely measure this property is not known.

Three failure models (linear-elastic fracture, elastic-plastic J-integral, and net-section plastic instability) have been compared to predict the critical criterion for the fracture of a 29-in. (73.7-cm) i. d., by 2.5-in. (6.35-cm) thick 316 stainless steel pipe. For the PWR hot leg under uniform axial loading, the critical failure criterion is the net-section plastic instability; i.e., when the average stress on the remaining ligament exceeds the material flow stress.

The potential energy definition of the J-integral was used to estimate J as a function of load for the elastic-plastic analysis. A linear elastic analysis of J, i.e., the stress intensity solution (in terms of J), provided a lower bound estimate of J, whereas a plastic-limit-load analysis gave an upper bound value. The results are self-consistent and appear realistic when compared with observed behavior.

Finally, the fracture requirement for a load source applied external to the pipe was evaluated. Using an energy approach, we found that the J-integral provided the lowest energy requirement. Using qualitative arguments, we estimated the energy requirement stored in the external source such that sufficient energy could be supplied to propagate pipe fracture.

## 5.0 REFERENCES


1. Lu, S., Streit, R., and Chou, C.K., Probability of a Pipe Fracture in the Primary Coolant Loop of a PWR Plant. Vol. 1: Summary, Lawrence Livermore National Laboratory, Livermore, CA, UCID-18967, Vol. 1, NUREG/CR-2189, Vol. 1 (1981).
2. Harris, D.O., Lim, E.Y., and Dedhia, D.D., Probability of a Pipe Fracture in the Primary Coolant Loop of a PWR Plant. Vol. 5: Probabilistic Fracture Mechanics Analysis, Lawrence Livermore National Laboratory, Livermore, CA, UCID-18967, Vol. 5, NUREG/CR-2189, Vol. 5 (1981).
3. Chan, A.,Lu, S. C., Rybicki, E. F. , and D. J. Curtis, Probability of a Pipe Fracture in the Primary Coolant Loop of a PWR Plant. Vol. 3, Nonseismic Stress Analysis,Lawrence Livermore National Laboratory, Livermore, CA, UCID-18967, Vol. 3, NUREG/CR-2189, Vol. 3 (1981).
4. Streit, R., Probability of a Pipe Fracture in the Primary Coolant Loop of a PWR Plant. Vol. 8: Pipe Fracture Indirectly Induced by an Earthquake, Lawrence Livermore National Laboratory, Livermore, CA, UCID-18967, Vol. 8, NUREG/CR-2189, Vol. 8 (1981).
5. Final Safety Analysis Report (FSAR), Zion Station, Unit 1, Commonwealth Edison Company.
6. "Code Allowable Stresses for Nuclear Piping Material," Boiler and Pressure Vessel Code, Sec. VIII (American Society of Mechanical Engineers, New York , 1980).
7. American Society for Testing and Materials, "The Determination of $J_{Ic}$, A measure of Fracture Toughness; Proposed Standard," ASTM Committee E24 (1980).
8. Mayfield, M.E., Forte, T.P., Rodabaugh, E.C., Leis, B.N., and Elber, R.J., Cold Leg Integrity Evaluation, Battelle Columbus Laboratories, Columbus, OH, NUREG/CR-1319 (1980).
9. American Society for Metals, Metals Handbook, Vol. 1, 8th ed., pp. 410-434.
10. Simmons, W.F. and Van Echo, J.A., Report on the Elevated-Temperature Properties of Stainless Steels, ASTM Data Series Publication DS5-S1, American Society for Testing and Materials (1965).

11. Smith, G.V., An Evaluation of the Yield, Tensile, Creep, and Rupture Strengths of Wrought 304, 316, 321, and 347 Stainless Steels at Elevated Temperatures, Prepared for tne Metals Properties Council, ASTM Data Series DS5-S2, American Society for Testing and Materials (1969).
12. Kadlecek, P., "Mechanical Property Data on Hot-Extruded 304N and 316N Stainless Steel Pipe," in Elevated Temperature Properties as Influenced by Nitrogen Additions to Types 304 and 316 Austenitic Stainless Steels, ASTM STP 522, ASTM, pp. 3-34, (1973).
13. Bamford, W.H., and Bush, A.J., "Fracture Behavior of Stainless Steel," in Elastic-Plastic Fracture, ASTM STP 668, ASTM, pp. 553-577, (1979).
14. Landerman, E.I., and Bamford, W. H., "Fracture Toughness and Fatigue Characteristics of Centrifugally Cast Type 316 Stainless Steel Pipe after Simulated Thermal Service Conditions," in Ductility and Toughness Considerations in Elevated Temperture Service, ASME, MPC-8 (1978).
15. Swindeman, R.W., McAfee, W.J., and Sikka, V.K., "Product Form Variability in the Mechanical Behavior of Type 304 Stainless Steel at Room Temperature and 593°C (1100°F)," in Reproductibility and Accuracy of Mechanical Tests, ASTM STP 626, American Society for Testing and Materials, pp. 41-64 (1977).
16. Stiansen, S.G., Mansour, A., Jan, H.Y., and Thayamballi, A., "Reliability Methods in Ship Structures," The Royal Inst. of Naval Arcn., Spring Mtg, 1979.
17. Goepfert, W.P., "Statistical Aspects of Mechanical Property Assurnace," Reproducibility and Accuracy of Mechanical Tests, ASTM STP 626, American Society for Testing and Materials, pp. 136-144 (1977).
18. Mischke, C.R., "Some Tentative Weibullian Descriptions of the Properties of Steels, Aluminums, and Titaniums," ASME, 71-Vibr-64 (1971).
19. Begley, J.A., and Landes, J.D., "The J Integral as a Fracture Criterion," in Fracture Toughness, Proceedings of the 1971 National Symposium on Fracture Mechanics, Part II, ASTM STP 514, American Society for Testing and Materials, pp. 1-20 (1972).
20. Paris, P.C., Tada, H., Zahoor, A., and Ernst, H., "The Theory of Instability of the Tearing Mode of Elastic-Plastic Crack Growth," in Elastic-Plastic Fracture, ASTM STP 668, J. D. Landes, J. A. Begley, and G. A. Clarke, Eds. (American Society for Testing and Materials, 1979) pp. 5-36.

21. Goldberg, A., Streit, R., and Scott, R., Evaluation of Cracking in the Feedwater Piping Adjacent to the Steam Generators in Nine Pressurized Water Reactor Plants, Lawrence Livermore National Laboratory, Livermore, CA, UCRL-53000, NUREG/CR-1603, pp. 169-186 (1980).

22. Nilsson, F. and Ostensson, B., "$J_{Ic}$-Testing of A-533B Statistical Evaluation of Some Different Testing Techniques," Engineering Fracture Mechanics 10, 223-232 (1978).

23. Harris, D.O., The Influence of Crack Growth Kinetics and Inspection on the Integrity of Sensitized BWR Piping Welds, Electric Power Research Institute, Palo Alto, CA, EPRI NP-1163, (1979).

24. Rice, J.R., "A Path Independent Integral and the Approximate Analysis of Strain Concentration by Notches and Cracks," J. Appl. Mech., 35, 379-386 (1968).

25. Hutchinson, J.W., "Singular Behaviour at the End of a Tensile Crack in a Hardening Material," J. Mech. Phys. Soilds, 16, 13-31 (1968).

26. Rice, J.R., and Rosengren, G.F., "Plane Strain Deformation Near a Crack Tip in a Power-Law Hardening Material," J. Mech. Phys. Solids, 16, 1-12, (1968).

27. McClintock, F.A., in Fracture, Vol. 3, H. Liebowitz, ed. (Academic Press, New York, 1971) pp. 47-225.

28. Landes, J.D., and Begley, J.A., "The Effect of Specimen Geometry and $J_{Ic}$," in Fracture Toughness, Proceedings of the 1971 National Symposium on Fracture Mechanics, Part II, ASTM STP 514, American Society for Testing and Materials, 1972, pp. 24-39.

29. Hallquist, J.O., NIKE2D: An Implicit, Finite-Deformation, Finite-Element Code for Analyzing the Static and Dynamic Response of Two-Dimensional Solids, Lawrence Livermore National Laboratory, Livermore, CA, UCRL-52678, (1979).

30. Roark, R. J., Formulas for Stress and Strain, (McGraw Hill, New York, 1954) 3rd ed., pp. 141-143.

31. Tada, H., Paris, P., and Gamble, R., Stability Analysis of Circumferential Cracks in Reactor Piping Systems, U.S. Nuclear Regulatory Commission, Washington, D.C., NUREG/CR-0838 (1979).

32. Irwin, G., University of Maryland, College Park, MD, private communication (1980).

# 6.0 GLOSSARY

Artificial accelerogram

A numerically simulated acceleration time-history plot of an earthquake's ground motion.

Aspect ratio

Half-length-to-depth ratio of a semi-elliptical surface crack, $D/a = \beta$ . The half length is measured along the surface of the pipe.

Availability

The percent of time that the reactor plant is actually in operation during its 40-yr life. For Zion, the estimated availability is 70%.

Boundary integral equation (BIE) technique

A mathematical solution of three-dimensional elasticity problems which divides a body's surface into elements and provides displacements and tractions at surface nodal points. Results are a set of simultaneous linear equations that are solved for the unknown nodal displacements or tractions.

BWR

Boiling water reactor.

Cold leg

Portion of the primary coolant loop piping which connects reactor coolant pump to reactor pressure vessel.

Conditional probability

If A and B are any two events, the conditional probability of A relative to B is the probability that A will occur given that B has occurred or will occur.

Confidence interval

An interval estimator with a given probability (the confidence coefficient) that it will contain the parameter it is intended to estimate.

Containment

A concrete shell designed to house the NSSS, the polar crane, and other internal systems and components of a nuclear power plant.

Correlation

The interdependence between two or more variables.

Couple

To combine, to connect for consideration together.

Covariance

The expected value of the product of the deviations of two random variables from their respective means. The covariance of two independent random variables is zero, but a zero covariance does not imply independence.

Crossover leg

Portion of the primary coolant loop piping which connects the steam generator to the reactor coolant pump.

Cumulative distribution function (cdf)

A function that gives the probability that a random variable, X, is less than or equal to a real value, x.

DEPB

Double-ended pipe break.

Decouple

The opposite of couple; disconnecting two events.

EPFM

Elastic-plastic fracture mechanics.

Estimate

A number or an interval, based on a sample, that is intended to approximate a parameter of a mathematical model.

Estimator

A real-valued function of a sample used to estimate a parameter.

Fatigue crack growth

Growth of cracks due to cyclic stresses.

Flow stress

The average of the yield strength and ultimate tensile strength of a material. Approximate stress at which gross plastic flow occurs.

Fracture

See pipe fracture.

Girth butt weld

Circumferential weld connecting adjacent pipe ends. The girth butt welds referred to in this report are in the primary coolant loop piping.

Hazard curve (seismic)

The probability that one earthquake will generate a specified value of the peak ground acceleration in a time interval of specified length, usually one year.

Hot leg

Portion of the primary coolant loop piping which connects the reactor pressure vessel to steam generator.

Independent events

Two events are independent if, and only if, the probability that they will both occur equals the product of the probabilities that each one, individually, will occur. If two events are not independent, they are dependent.

Independent random variables

Two or more random variables are independent if, and only if, the values of their joint distribution function are given by the products of the corresponding values of their individual (marginal) distribution functions. If random variables are not independent, they are dependent.

LEFM

Linear-elastic fracture mechanics.

Large LOCA

Large loss-of-coolant accident. For the purpose of this report the large LOCA is equivalent to a pipe fracture in the primary coolant loop pipe. (See pipe fracture).

Leak-before-break situation

A pipe defect that grows to become a through-wall crack but is of insufficient length to result immediately in a complete pipe severance.

Load-controlled stress

Stress upon a pipe that cannot be relaxed by displacement. As such, the load is not relieved by crack extension. In this analysis pressure, dead weight, and seismic stresses are assumed to be load controlled.

Mean

(1). A measure of the center of a set of data. The sample mean of n numbers is their sum divided by n. (2). A population mean is a measure of the center of the probability density function. This is also called the mathematical expectation.

NSSS

Nuclear steam supply system.

OBE

Operating basis earthquake.

Operating stress

Stress in the piping due to normal operating loads, e. g., dead weight, pressure, start ups, etc.

Pipe fracture

A double-ended guillotine pipe break; also referred to in this report as a LOCA and a large LOCA. Refers to a circumferential pipe fracture in which pipe sections on either side of the fracture are completely severed from each other.

Pipe severance

See pipe fracture.

Poisson process

A random process, continuous in time, for which the probability of the occurrence of a certain kind of event during a small time interval t is approximately $\lambda t$, the probability of occurrence of more than one such event during the same time interval is negligible, and the probability of what happened during such a small time interval does not depend on what happened before.

PRAISE

A computer code, Piping Reliability Analysis Including Seismic Events, developed to estimate the time to first failure for individual joints in a piping system. It is used to analyze the Zion 1 primary coolant loop. PRAISE is written in FORTRAN.

Primary cooling loop

Cold leg, hot leg, and crossover leg.

Probability density function (pdf)

A non-negative, real-valued function whose integral from a to b (a less than or equal to b) gives the probability that a corresponding random variable assumes a value on the interval from a to b.

PWR

Pressurized water reactor.

Radial gradient thermal stress

Axisymmetric stress in the pipe arising from temperature variations through the pipe wall thickness. In this report, the radial gradient thermal stress is a result of temperature transients in the reactor coolant.

Random variable

A real-valued function defined over a sample space, by a probability distribution.

Response spectrum analysis

A response analysis that estimates the maximum response from response spectra.

RCL

Reactor coolant loop.

RCP

Reactor coolant pump.

Risk

Expected loss.

RPV

Reactor pressure vessel.

Sample space

A set of points that represent all possible outcomes of an experiment.

S factor

Stress factor used for fatigue analysis to account for multiple stress cycles.

Seismic hazard curve

See hazard curve.

SG

Steam generator.

Simulation

Numerical technique employed to simulate a random event, artificial generation of a random process. The PRAISE computer code uses Monte Carlo Simulation to estimate the probability of failure in nuclear reactor piping.

Soil impedance functions

Forces required to oscillate the foundation through unit displacements in different directions.

SSE

Safe shutdown earthquake.

Standard deviation

(1). A measure of the variation of a set of data. The sample standard deviation of a sample of size n is given by the square root of the sum of the deviations from the mean divided by (n-1). (2). A measure of the variability of a random variable. The population standard deviation is the square root of the variance; the mean of the square of the random variable minus its mean.

Statistically dependent

Two events are statistically dependent if they do not fit the criterion for statistical independence.

Statistically independent

See independent events.

Stratified random sampling

A method of sampling in which portions of the total sample are allocated to individual subpopulations and randomly selected from these strata. The principal purpose of this kind of sampling is to guarantee that population subdivisions of interest are represented in the sample, and to improve the precision of whatever estimates are to be made from the sample data.

Stress corrosion cracking

Cracking due to the combined effects of stress and corrosion.

Stress intensity factor

A fracture mechanics parameter that describes the state of steam at the tip of a crack.

Surge line

Piping that connects pressurizers to the reactor coolant loop. In the Zion I PWR the surge line is a branch from the hot leg in Loop 4.

Time-history response analysis

A response analysis that estimates the maximum response from response spectra.

Transient

An event in the operation of the PWR that gives rise to a load in the piping over a specified length of time.

Uncertainty

Absence of certainty due to randomness of a random variable or lack of knowledge of the edf of a random variable.

Uniform hazard method (uhm)

A procedure for estimating frequency of occurrence distributions for various ground motion parameters.

UT

Ultrasonic testing.

Variance

The mean of the squares of the deviations from the mean of a random variable.

ZPGA

Zero period ground acceleration; defines the size of an earthquake.